



IRI Performance Models for Flexible, Semi-Rigid and Composite Pavements in Double-Carriageway Roads

Itziar Gurrutxaga ¹, Ángela Alonso-Solórzano ², Miren Isasa ¹, Heriberto Pérez-Acebo ^{3*}

¹ Department of Mechanical Engineering, University of the Basque Country UPV/EHU, Donostia-San Sebastián, Spain.

² Department of Physics, University Francisco de Vitoria, Carretera Pozuelo-Majadahonda, Pozuelo de Alarcón 28223, Spain.

³ Department of Mechanical Engineering, University of the Basque Country UPV/EHU, Bilbao 48013, Spain.

Received 13 January 2025; Revised 18 April 2025; Accepted 22 April 2025; Published 01 May 2025

Abstract

Pavement Management Systems (PMS) depend upon reliable pavement performance models. In this paper, our aim is to develop International Roughness Index (IRI) prediction models for the heavily trafficked (right-hand) lanes of motorways in the province of Gipuzkoa (Spain) in flexible, semi-rigid, and composite pavements. A deterministic approach was selected, based on the available information in the PMS employed in that province, covering complete pavement structures. Omitting pavement type, the model yielded a determination coefficient (R^2) of 0.696 with only three variables: pavement age, cumulative volume of heavy vehicles travelling through the section, and total thickness of bituminous layers. Then, two superior models were generated with pavement type as a variable, yielding R^2 values of 0.781 and 0.795, respectively. Unlike the opaque features of Machine Learning (ML), the deterministic models captured precise relationships between the variables to a high degree of accuracy. They can moreover be applied to all pavements with bituminous layers, unlike many other models that are only applicable to a single pavement type. Furthermore, the models are presented for freeways where traffic is randomly distributed between lanes; a less widely covered topic in the literature.

Keywords: International Roughness Index; Pavement Performance Model; Flexible Pavement; Semi-Rigid Pavement; Composite Pavements.

1. Introduction

Road pavement structures consist of layers of graded materials that are normally referred to as surface, base, and subbase (the latter at times unnecessary), all resting upon a compacted subgrade [1]. Together, all the layers create a robust foundation that can withstand vehicular traffic and environmental stress [2]. There are at present two main pavement surfaces: Portland cement concrete and bituminous materials, usually referred to as asphalt concrete. Pavements may therefore be categorised as either rigid or flexible, respectively [3]. Rigid pavements have a concrete slab poured over a subbase layer of either granular or stabilised materials. Flexible pavements have a layer of asphalt mix over unstabilised aggregates [4, 5], the latter category representing approximately 95% of all road networks throughout the world [3].

The load transmission of each pavement type differs, regardless of the different surface materials and subsequent treatments. The general objective is to ensure that the subgrade materials will withstand the stress distribution patterns. The high degree of stiffness of the concrete slab enables it to carry most of the load [6], so the stress concentrations of the underlying layers are in that way minimised. In contrast, traffic loads over the surface layer of a flexible pavement

* Corresponding author: heriberto.perez@ehu.eus

<http://dx.doi.org/10.28991/CEJ-2025-011-05-01>



© 2025 by the authors. Licensee C.E.J, Tehran, Iran. This article is an open access article distributed under the terms and conditions of the Creative Commons Attribution (CC-BY) license (<http://creativecommons.org/licenses/by/4.0/>).

result in deformation of the base material of unstabilised aggregates. At greater depths, loads are distributed over larger areas, so high-intensity stress levels that are generally recorded close to the surface subsequently diminish at deeper layers [7, 8]. It is therefore essential to utilise the highest quality materials at the surface, incorporating lower quality materials at deeper layers [4]. Nevertheless, as traffic volumes are constantly increasing, pavements are required to withstand ever higher stresses and more frequent loading cycles, which can result in permanent deformation of granular bases and asphalt surface layers [2, 9]. Treatments to enhance base-layer performance include a variety of methods and the following materials: cement, lime, bituminous materials, recycled asphalt pavement, fly ash, slag, and calcium chloride [8, 10-13]. Treated or stabilised base materials increase the strength of the pavement structure and broaden load distribution over wider areas, thereby diminishing subgrade stress levels [14]. Pavements comprising an asphalt mixture layer or layers over a treated base or subbase are categorised as semi-rigid pavements [15-17]. Semi-rigid pavements may be categorised as an intermediate type somewhere between flexible and rigid pavements, although their behaviour is always closer to flexible rather than rigid pavements [18].

The composite pavement is the last pavement type, formed of a bituminous layer placed over a Portland cement concrete base. Its construction method combines the durability and strength of concrete with the flexibility and smoothness of an asphalted surface. In this pavement type, an asphalt mixture layer or layers are extended over a Portland cement concrete base [4]. Often used for the rehabilitation of Portland cement concrete pavements at the end of their functional lifespan, the surface is overlaid with Hot-Mix Asphalt (HMA) layers. The extension of HMA layers is a standard maintenance treatment for rigid pavements in the U.S. Midwest [19, 20]. As well as its use in roadways, this technique is usually applied over concrete structures, such as bridges, where the concrete base constitutes part of the overall structure. The robust support of a composite pavement ensures that a bridge can withstand significant loads and environmental weathering. The bituminous layer also introduces flexibility and enhances surface characteristics, such as improving skid resistance, which is vital for vehicle safety [21]. It is a combination that effectively distributes loading while absorbing thermal expansion and contraction, which is of particular importance in bridge applications.

Although pavements are designed as *per* the relevant standards, deterioration is inevitable over time, due to a number of factors, including traffic loads, material ageing, environmental factors, and construction deficiencies [22-27]. Given that the total cost of maintenance and rehabilitation (M&R) works is generally higher than available funds, road agencies must implement Pavement Management Systems (PMS) for optimal budgeting and maintenance planning [28-31]. According to AASHTO [32], a PMS is “*a set of tools or methods that assist decision makers in finding optimum strategies for providing, evaluating, and maintaining pavements in a serviceable condition over a period of time*”. A PMS therefore relies upon: 1) data collection procedures to assess current pavement conditions; 2) the forecasting of future conditions using pavement performance or deterioration models; and 3) the development of customised maintenance strategies considering local characteristics and traffic, available materials and funding [28, 32-34].

Highway agencies employ various indices directly measured on the road network in their evaluations of pavement conditions. Although the surface merely corresponds to one layer of the pavement structure, it is the layer in contact with the tyres of a travelling vehicle and is therefore of paramount importance. Cracking, potholes, rutting, ravelling, depressions, pavement strength, and drainage can all worsen surface roughness [35]. In turn, surface roughness has a direct influence on Vehicle Operating Costs (VOC), user comfort and safety, road maintenance costs, and service life [36-40]. Among the numerous indices for pavement roughness assessment, including the Present Serviceability Index (PSI) and Present Serviceability Rating (PSR), the International Roughness Index (IRI) is the most widely used [27, 41]. The IRI was an unanticipated outcome of the International Roughness Experiment conducted in Brazil in 1982, and the World Bank went on to develop it during the 1980s [42, 43]. Sayers [44] devised the algorithm that is used to calculate the IRI, which represents the accumulated suspension stroke of a vehicle divided by the distance travelled, expressed in mm/m or m/km. The stability of the IRI over time and its transferability throughout the world are all reasons for its extensive global use [45]. Examples of its employment can be found in both developed [46-49] and developing countries [50-53].

In the province of Gipuzkoa (Spain), the Provincial Council of Gipuzkoa (PCG) is responsible for the management of motorways (freeways) and interurban highways, while local councils assume responsibility for the management of local roads. The PCG manages a comprehensive network of over 1,100 km of roadways. Similar to other highway agencies, it collects IRI values in order to evaluate the current condition of the road network. The information is stored on the agency database together with other inputs to the PMS, such as traffic volumes, pavement structures, M&R activities, climate data, *etc.* [54].

Taking advantage of this information, the objective of this paper is to present a comprehensive IRI prediction model for dual-carriageways, specifically freeways, and multilane highways. The model encompasses all potential pavement structures in Gipuzkoa, including flexible, semi-rigid, and composite pavements. It was developed for the right-hand lanes of dual-carriageways; the lanes on which most heavy vehicles circulate and therefore the lanes that deteriorate more rapidly than any other. Highway agencies need to know the condition of the right-hand lane to carry out M&R works in proper time. The model is based on a rigorous selection of variables that, as has been demonstrated, exert significant influence on IRI performance.

The structure of this paper is organised as follows. In the following section, the state-of-the-art pavement deterioration models classified by pavement type are presented with a special focus on motorways. Then, the information registered in the PMS of the PCG, a discussion of the methodology and a list of the selected variables for modelling are all presented in Section three. In the fourth section, the results are detailed and discussed. Finally, the conclusions are drawn in the last section.

2. Literature Review

2.1. Classification of Pavement Performance Models

Pavement performance models, also known as pavement deterioration models, evolution models, deterioration models, and pavement performance prediction models, all serve as mathematical frameworks to foresee changes to pavement characteristics over specified periods of analysis [55, 56]. A wide variety of pavement performance models is available, as well as various classifications and categories within which to group those model types. For example, Haas et al. [57] firstly grouped the models that road agencies developed for pavement management into four fundamental categories: purely mechanistic, mechanistic-empirical, regression (or deterministic), and subjective (which included probabilistic models, as the latter were sometimes subjectively developed). In a more recent publication, the Pavement Management Guide [54], the models are categorised in four distinct groups: deterministic, probabilistic, Bayesian, and subjective (or expert-based). Some years earlier, Uddin [58] had proposed that, in addition to deterministic and probabilistic models (which included Markov chains and Bayesian models), a further category, the Artificial Neural Network (ANN), should also be considered. Over more recent years, interest has been growing in the use of ANN models and, more generally, Machine Learning (ML) models for the prediction of pavement performance. The broad variety of ML models has a series of classifications. For instance, Justo-Silva et al. [59] classified them into three basic groups: supervised learning, unsupervised learning, and reinforcement learning. Nevertheless, despite the wide range of available models, deterministic and probabilistic models are still regarded as the fundamental groups [26, 49, 60-62].

The deterministic model is useful whenever data on historical pavement conditions and adequate survey data can be used to identify patterns of deterioration. Regression analysis is typically applied in the development process. Deterministic models, of proven efficiency for large experimental and historical datasets [51, 63], establish both linear and nonlinear relationships between affecting factors and the predicted variable, offering simplicity and reliability [62, 64]. However, their utility is constrained by their inability to extrapolate beyond the limits of experimental data [65], and they need to be calibrated when applied to an alternative site.

Unlike the precise index values of the deterministic model, the probabilistic model generates an estimate of the probabilistic distribution of the expected values [52, 66]. Both models predict future conditions, although inherent uncertainties over future pavement conditions can be built into probabilistic models [26, 67]. In fact, pavement deterioration is now understood as probabilistic in nature with some uncertainty levels [26, 68, 69]. Over the past three decades, various forms of probability-based models have emerged, and Bayesian and Markov probabilistic models have attracted significant interest [49, 60, 70-72].

Machine learning models for empirical modelling are also gaining ground, employing parallel computations for knowledge representation and processing [59, 73]. Capable of solving complex problems that traditional approaches cannot, they require significant amounts of data [27, 74-76]. Nonetheless, their results are not easily interpreted, as their "black box"-type definitions establish no clear causal relationships between inputs and outputs [49, 77, 78]. A drawback that limits transferability to other regions or countries.

Subjective or expert-based models that integrate subjective opinions into performance modelling are less formal. They are suitable whenever historical data are limited and new practices or materials must be introduced.

2.2. IRI Performance Models for Flexible Pavements

Flexible pavements that consist of bituminous layers spread over an unbound material base are common road surfaces around the world [3]. Hence, the first pavement performance models were designed for that pavement type. Initially, empirical approaches were used to establish relations between pavement roughness and various affecting factors. Among the earliest, the AASHO model [79] listed the material properties and the thicknesses of the layers, subgrade strengths, and environmental data for estimating the maximum number of Equivalent Single Axle Load (ESAL) applications. After developing the IRI, the World Bank published HDM-III [80] and HDM-IV [81], which contained some of the first models. The model proposed by Paterson [82] can be used to identify the main variables affecting the IRI: cracking, potholing, rutting, structural deformation (caused by traffic loads), and weathering. In general, it could be said that there has been a shift away from empirical models to more complex mechanistic-empirical (M-E) models, *i.e.*, linking theoretical mechanics with empirical data to improve accuracy [83]. A leading example of this transition is the Mechanistic-Empirical Pavement Design Guide (MEPDG) that AASHTO [84, 85] proposed, as an outcome of the National Cooperative Highway Research Program (NCHRP) 1-37A [86]. The models used in North

America for pavement structures with equations for various distress types are presented in the MEPDG. The following Equation 1 is proposed in the IRI for Hot Mix Asphalt pavements and Hot Mix Asphalt overlays over flexible pavements:

$$IRI = IRI_0 + 40.0 \cdot RD + 0.4 \cdot FC_{Total} + 0.008 \cdot TC + 0.015 \cdot SF \quad (1)$$

where IRI is the predicted IRI value (in./mi.); IRI_0 is the initial IRI after construction (in./mi.); RD is the average rut depth (inches); FC_{Total} is the area of fatigue cracking (combining longitudinal, alligator cracking, and reflection cracking along the wheel path), as a percentage of total lane area; TC is the length of transverse cracking, including the reflection of transverse cracks in existing HMA pavements (ft/mi); and SF is the site factor, obtained from Equation 2:

$$SF = Age^{1.5} \cdot \{ \ln[(precip + 1) \cdot (FI + 1) \cdot p_{02}] \} + \{ \ln[(precip + 1) \cdot (PI + 1) \cdot p_{200}] \} \quad (2)$$

where Age is the pavement age (years); $precip$ is the annual precipitation (inches); FI is the average annual freezing index ($^{\circ}F$); PI is the plasticity index of the soil; and p_{02} and p_{200} are the respective percentages that pass through the 0.02 and the 0.075 cm sieves. The proposed model, Equation (1), yielded a determination coefficient (R^2) of 0.56 with 1926 data points, and a standard error of the estimate (SEE) of 0.298 m/km (18.9 in./mi.).

Abdelaziz et al. [87], Pérez-Acebo et al. [88] and Sandamal et al. [27] presented a set of tables with some IRI prediction models for flexible pavements. The listed models covered a wide variety of variables, which could be classified as age, climate factors, distress (mainly rutting, potholes, and cracking), initial IRI, traffic volumes, and soil and material parameters (mainly structural numbers and material characteristics) [87-91]. Wu et al. [62] also employed similar variables in their most recently developed models. Likewise, Shokoohi et al. [26] included data on cumulative annual freeze-thaw cycles, cumulative annual precipitation rates (climate factors), cumulative ESAL in one direction (traffic factor), Structural Numbers (structural index), initial IRI and pavement age. Similarly, Marcelino et al. [92] used climate factors (temperature, precipitation, freezing index), and traffic and material properties for predicting future IRI values. Kaloop et al. [93] advanced eight variables: initial IRI, pavement age, distress indices, freeze index and material properties. Using data from Korea, Choi & Do [94] fed traffic, climate and distress data into their prediction model. Sandamal et al. introduced data on pavement age and traffic volume as their variables [27]. Moreover, Nguyen et al. developed an IRI performance model in Vietnam with no other data than distress indices [95]. As previously mentioned, factors such as pavement age, traffic loads, pavement material properties, and environmental factors were among the key variables included in all the above models. Additionally, as shown by Kaloop et al. [93], it must be noted that at present, there is a trend to develop deterioration models for flexible pavements using data from the LTPP where many variables are available. However, many other highway agencies have far less data and far fewer variables recorded, so there is a need to develop specific models that include the variables that highway agencies apply in their own PMS.

2.3. IRI performance Models Applied to Semi-Rigid Pavements

Over recent years, the use of treated base materials that are laid under semi-rigid pavements has been popularised, especially in China, where high traffic demand drives the construction of this more resistant type of pavement [16, 17, 96]. Despite the immense effort invested in characterising the treated materials of semi-rigid pavements [16, 97-99], few IRI performance models have been developed for this pavement type. Despite the IRI models for flexible pavements that were presented in the first and second versions of the MEPDG [84, 85], neither version included models for semi-rigid pavements. However, a model for semi-rigid pavements did appear in the third version of the MEPDG [100], which is shown below as Equation 3:

$$IRI = IRI_0 + 40.8 \cdot RD + 0.575 \cdot FC_{Total} + 0.0014 \cdot TC + 0.00825 \cdot SF \quad (3)$$

where IRI , IRI_0 , RD , FC_{Total} and TC are defined in Equation 1, and SF is a site factor defined in Equation 2.

Pérez-Acebo et al. [101] presented two IRI prediction models specifically developed for semi-rigid pavements. The first one, shown in Equation 4, yielded a determination coefficient (R^2) of 0.569:

$$IRI = 2.22 + 0.22 \cdot \ln(R.Age) - 1.16 \cdot 10^{-6} \cdot TotVeh \cdot TotBit + 1.87 \cdot 10^{-4} \cdot TotH.Veh + BASE \cdot Bthick \quad (4)$$

where IRI is the predicted IRI (m/km); $R.Age$ is the real pavement age (years); $TotBit$ is the thickness of the bituminous layers (cm); $TotVeh$ and $TotH.Veh$ represent the total numbers, respectively, in thousands of vehicles and heavy vehicles that travel over the section; $BASE$ is a variable that considers the materials used in the treated base; and $Bthick$ is the thickness of the treated base layer (cm).

An improved model that incorporated the variable $SURF$, an estimate of surface-layer bituminous material, was also presented in Pérez-Acebo et al. [101], as shown in Equation 5, that yielded an R^2 of 0.645.

$$IRI = 1.397 + 0.184 \cdot \ln(R.Age) - 7.72 \cdot 10^{-7} \cdot TotVeh \cdot TotBit + 1.88 \cdot 10^{-4} \cdot TotH.Veh + BASE \cdot Bthick + SURF \quad (5)$$

where the rest of variables are as defined for Equation 4.

Using data from the LTPP, Hanson [102] proposed Equation 6 for IRI predictions relating to semi-rigid pavements with varied volumes of cement in the treated base layer:

$$IRI = 1.0 + 0.019t - 0.00832a + 0.0072b + 0.0346c \quad (6)$$

where IRI is the predicted IRI value (m/km); t is the pavement age (years); a is the thickness of the asphalt concrete layer (cm); b is the thickness of the cement-treated base (cm); and c is the cement content (%). However, Equation 6 yielded a very low R^2 of 0.09.

Assogba et al. [103] studied the mechanical response of three semi-rigid sections under traffic load and nonlinear temperature gradients. The results of an initial Finite Element Method (FEM) analysis were verified in a full-scale track pavement test. It was observed that the non-linear thermal gradient of the pavement temperatures and the contact condition of the interfaces significantly affected both the stress and the strain patterns within the pavement system. Both the FEM and the in-situ results of Yang et al. [96] demonstrated that with higher resilient moduli in the base materials (i.e., semi-rigid pavements), the rutting of the asphalt and base layers was reduced, but when only considering surface layer rutting, more resilient materials at the base implied higher deformation levels. Dong et al. [16] noted that the stiffness of the base materials pre-treated with cement had slightly increased after 10 years, although it had decreased in base materials treated with lime and fly ash. They also developed a fatigue model that was restricted to a specific structure.

Although those studies [16, 96, 103] represent important advances in the characterisation of semi-rigid pavements, there are still no specific models for predicting future IRI values other than those presented in Equations 3 to 6. Consequently, more IRI prediction models must be developed for semi-rigid pavements.

2.4. IRI Performance Models for Composite Pavements

Composite pavement prediction models have mainly been developed in the U.S., due to their frequent use as rehabilitation solutions for PCC pavements. Khattak et al. [19] presented an IRI prediction model for composite pavements (asphalt-overlay over concrete) in the state of Louisiana. Their deterministic (regression analysis) model yielded R^2 values of 0.63, using nine variables: pre-treatment IRI value, HMA, and PCC layer thicknesses, cumulative ESAL, functional classification, treatment age, cumulative temperature index, precipitation index, and a variable delta. Using data from the LTPP, Barros et al. [104] compared five ANN models and the best performing ones used 14 input variables, including initial IRI, climate factors, asphalt and concrete thicknesses, and traffic loads, yielding an R^2 of 0.88. Moreover, Barros et al. [105] also compared an ANN and a Multiple Linear Regression (MLR) model for IRI prediction in the context of composite pavements within the wet non-freeze climate zone of the LTPP with 11 variables, including Initial IRI, age, material properties and climate factors. The R^2 values of the MLR and ANN models increased to 0.37 and to 0.86, respectively. After data clustering the composite pavement section characteristics on the LTPP database into three groups, Neema [106] applied Markov chain analysis and Monte Carlo simulation to develop a performance model for each cluster. Using this family of models to map trends of deterioration, flooding was incorporated to predict pre-and-post flood IRI values in affected sections. Some authors compared various model types (generally deterministic and ANN models) for predicting composite pavements, such as Kaya et al. [107] for pavements in Iowa (U.S.) and Abdelaziz et al. [87] using LTPP databases, in both cases with better results for the ANN models. As shown in Equation 3, the MEPDG [84, 85, 100] also contains a model for composite pavements, which is the same as for semi-rigid pavements.

Most of the models for composite pavements are used in the US and reflect the local characteristics of that technique. The localisation of the models adds to the need to develop models for other countries that are capable of capturing regional particularities.

2.5. IRI Performance Models for Freeways

There are many models for forecasting the IRI of different (mainly flexible) pavements types. Nevertheless, none have been specifically developed for the various lanes of dual carriageway roads, such as freeways and multilane highways. When researchers employ data from the LTPP, the highway characteristics are never indicated. However, as heavy vehicles are not uniformly distributed between the lanes of the carriageway, different pavement deterioration patterns may be expected. Some models are expressly indicated for single carriageway roads [88, 90]. However, very few have been explicitly developed for dual-carriageway highways. Al-Suleiman & Shiyab [108] developed a specific model for the slow (right-hand) lane -Equation 7-, in which heavy vehicles circulate more often, and another one for the faster (left-hand) lane -Equation 8-, both as an exponential function of pavement age, yielding determination coefficients of 0.801 and 0.61, respectively:

$$IRI_s = 0.796 \cdot e^{0.0539 \cdot Age} \quad (7)$$

$$IRI_f = 0.824 \cdot e^{0.0359 \cdot Age} \quad (8)$$

where IRI_s is the IRI value in the slow lane, IRI_f is the IRI value in the fast lane, and Age is the pavement age since construction or last overlay.

Georgiou et al. [109] developed an ANN model and a Support Vector Machine model for predicting IRI values on the heavy-trafficked slow lane of a high-volume motorway, obtaining slightly better accuracy with the ANN model.

In summary, while multiple models have been developed for flexible pavements, very few have been advanced for semi-rigid and composite pavements. Composite pavement sections are mainly constructed in the U.S., reflecting their local particularities. There is therefore a need to continue research on modelling semi-rigid pavements in general and composite pavements outside the US. However, there is no global model that includes all three pavement types. Additionally, very few models have been specifically produced for freeways where performance levels of the various lanes differ, as heavy traffic is never uniformly distributed between all the lanes. With the aim of bridging those two gaps identified in the literature, a complete IRI performance prediction model was developed in the present research for three possible road structures: flexible, semi-rigid and composite pavements for the right-hand lane of freeways using the data held on the PMS of the Provincial Council of Gipuzkoa (PCG).

The methodology proposed to develop this model is shown in Figure 1.

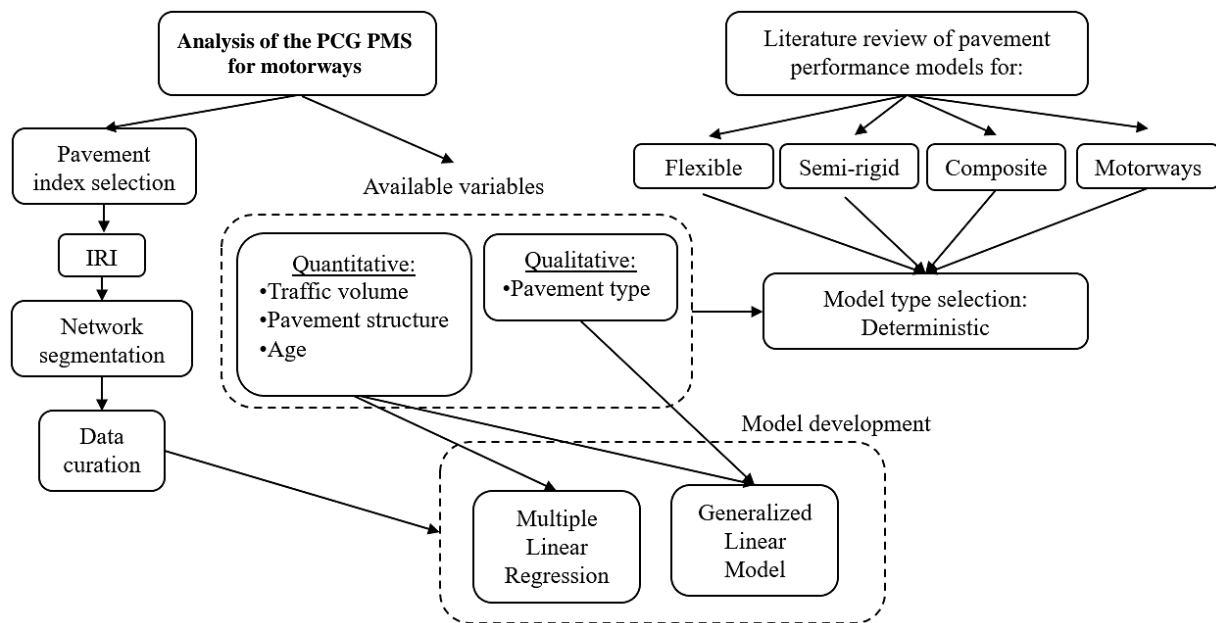


Figure 1. Flowchart of the proposed methodology

3. Data, Methodology, and Variables

3.1. The Data Held on the Pavement Management System of the Provincial Council of Gipuzkoa

Gipuzkoa, located in the north of Spain, is one of the three provinces of the autonomous region of the Basque Country. Its population stands at approximately 726,000. Its surface area, covering some 1,997 km², makes it the smallest province in Spain. Due to their special autonomous status, the provincial councils of the three Basque provinces are in charge of all road infrastructure, including all the highways and motorways (freeways), even those that form part of the long corridors connecting the provinces to other regions and to France. The PCG is therefore responsible for the management and maintenance of the province's complete interurban road network, excluding municipal roads. As a result, the PCG manages over 1,100 kilometres. It has implemented a comprehensive Pavement Management System (PMS) and collects the full range of infrastructural data on culverts, bridges and drainage installations, as well as geometric specifications (detailing carriageway configurations and interchange layouts) and exhaustive road and segment identification records throughout the network. In addition, the PCG compiles traffic data: Annual Average Daily Traffic, and the percentage of heavy vehicles. On that basis, the Annual Average Daily Traffic of heavy vehicles is calculated and published in an annual report online [110]. According to the Spanish standard [111], the maximum authorised weight of a heavy vehicle is at least 3,500 kg.

Besides, the PCG also incorporates environmental data into its PMS. Nevertheless, the decision not to include climatic data in the model was taken due to the relatively small surface of Gipuzkoa (1,997 km²) and the homogeneous oceanic climate throughout the province, which meant that climate-related data were not considered an affecting factor. In small areas with homogeneous climatic conditions, environmental data show little variance and are, therefore, not generally included in regional pavement modelling [101].

Furthermore, information on the pavement structures of new roads and the maintenance and rehabilitation (M&R) activities of the PCG over the last two decades are also added to the PMS. The PCG works to maintain a comprehensive dataset encompassing project parameters and pavement specifications. Each project entry records project details, pavement features, and material specifications, providing a solid basis for planning and maintaining the road infrastructure.

Finally, the PCG records pavement condition data, including indices on roughness, skid resistance, structural integrity, and surface defects, in order to maintain an overall picture of the state of the roads. Specifically, pavement roughness is collected by means of the International Roughness Index (IRI). IRI data are collected on an intermittent rather than on an annual basis. Data collected between 2018 and 2021 represent the only available data on the entire road network. IRI values are registered during summer and are reported at 100-metre intervals along the road, with precise initial and final Kilometre Point (KP) markers. For single-carriage dual-direction roads, IRI values are provided for both the right and left-hand lanes, while for double-carriageway roads only the IRI values for the right-hand lane are detailed in both directions. Thus, IRI prediction models for dual carriageways, as analysed in the present study, are models that have been specifically developed for the right-hand lane, which is the slowest lane with the heaviest traffic and, hence, the one that will need to be repaired before any other.

3.2. Applied Methodology

Given the extensive dataset within the PCG PMS database, including IRI values at 100-meter intervals, information on pavement structures, and annual traffic volumes of light and heavy vehicles, deterministic modelling was considered appropriate. A type of model that incorporates statistically significant variables for predicting IRI values on flexible, semi-rigid, and composite pavements. The model description discussed in the previous section implies the rejection of expert-based models, due to the inherent subjectivity of those models, and the availability of large data sets, suggesting alternative methodologies. Probabilistic models, including Bayesian and Markov chain models, were similarly discarded, because a different model for each unique factorial combination had to be developed, resulting in a large quantity of models. Furthermore, the superior accuracy of ML algorithms and Artificial Neural Networks (ANN) compared to deterministic models [26, 87] is acknowledged, with determination coefficient (R^2) values over 0.90, and even over 0.95. Between both groups, ML models rather than ANN models with tabular data are preferred [112, 113]. Nevertheless, both models were omitted due to the opaque characteristics of their results [49, 78]. A further objective of the research was to verify the feasibility of developing high accuracy model, which could clearly show the influence of each factor. When ML or ANN models are presented, other researchers or technicians of highway administrations cannot directly test the new models with their own data, because the model is unknown. Consequently, an additional output of the study was to provide an equation that can be used directly by any other road administration with similar weather patterns and, hence, a deterministic approach was selected.

Various curve types are used in deterministic models for data fitting, including linear, quadratic, cubic, logarithmic, and other functional forms, each displaying distinct patterns. While a single variable may be sufficient for a prediction model, multiple variables are commonly introduced, leading to the utilisation of MLR models. MLR is used to analyse interrelations between a quantitative dependent variable (the predicted variable) and various quantitative independent variables (the predictors or predicting variables), defined by known values. Moreover, qualitative predictors may be incorporated after their transformation into quantitative variables. Several hypotheses that assure post-model validation and development are assumed in the MLR analysis [90, 114, 115]:

- Linear association between dependent and independent variables. Tested with the Pearson coefficient (R), if the coefficient is low, then the variables can be transformed.
- Observation independence: each data point must be drawn independently from the population, which implies that errors are independent between them. A fact that can be checked with the Durbin-Watson statistic, ranging between 0 and 4. A value of 2 represents total independence, and values between 1.25 and 2.75 imply independent errors.
- Homoscedasticity: implying that the variance of errors must be equal across all levels, not depending on the observation. Homoscedasticity can be verified in a plot of the standardised predicted values vs. the standardized residuals, if no patterns are seen.
- Normal distribution of errors. Residuals must follow a normal distribution.
- Minimal or no multi-collinearity in the dataset, checked with the Variance Inflation Factor (VIF). If the VIF is over 10, the model has a serious multi-collinearity problem.

Moreover, the most general form of linear regression modelling is the Generalised Linear Model (GLM), a regression model that covers both MLR models with quantitative predictors and MLR models that use both quantitative and qualitative predictors. It is a broad framework that includes all Analysis of Variance (ANOVA) and Analysis of Covariance (ANCOVA)-related models.

3.3. Model Variables

In this section, the selection of the IRI prediction model variables is described in the light of PCG data.

As shown in the literature review, the most commonly used IRI prediction model variables cover pavement age (measured in years since construction or the last M&R work), traffic volumes, and structural parameters, which include information on the materials and the material properties of the section [62, 87, 88]. Given the significance of the pavement structures and their thicknesses and properties, only those pavement sections where the entire structure was documented were considered worth analysing—specifically, sections where the surface layer, base, and subbase were known, excluding the subgrade. So, the IRI model for deterioration only included fully documented sections. A comprehensive analysis was conducted on a road-by-road basis, focusing on road segments with well-defined pavement sections. Information on those segments was collected from the time they were opened to traffic until M&R activities were performed. The influencing variables for inclusion in the deterministic model were as follows:

- **Age.** Pavement age is commonly used for roughness modelling. [26, 93, 116]. It was, therefore, included in the analysis in two difference ways: “Age” and “RealAge”. The former variable represents the difference between the calendar year when the road section opened to traffic (or the most recent M&R activity) and the year of data collection (2018 and 2021). Since those dates can vary throughout the year, the latter variable was also incorporated. So, “Real Age” provided a more precise measurement of pavement age, taking into account the exact dates both of the road opening (or the most recent M&R activity) and of data collection. Expressed in years with a decimal fraction, a real age of 0.5 corresponds to six months. Pavement age expressed as a number of years with a decimal fraction can be found in other studies, among which [26].
- **Traffic Volume.** Traffic volume is generally incorporated into IRI models using the Equivalent Single Axle Load (ESAL), which standardises the damage caused by various vehicle weights to the damage caused by a standard load [26, 84, 92]. In Spain, the ESAL standard load is 13 tonnes. However, the specific numbers of each vehicle type passing through each section are not recorded in Gipuzkoa, as traffic data only differentiate between light and heavy vehicles. So, the following variables were included as potential influencing factors to account for traffic volumes.
- **Annual Average Daily Traffic (AADT):** the AADT of the year of IRI data collection (2018 or 2021). It refers to bidirectional AADT and to vehicles/day. A further variable, AADTprev, referring to the year preceding data collection (2017 and 2020) was also considered.
- **Annual Average Daily Traffic of Heavy Vehicles (AADT-HV):** the AADT of heavy vehicles, measured as heavy vehicles/day, in both directions. A further variable, AADT-HVprev referring to the preceding year of data collection was also considered.
- **Total Vehicles (TotalVeh):** the number of vehicles travelling on a road segment since it was opened or since its most recent M&R activity. Expressed as millions of vehicles, it takes into account the AADT of each year since the segment of road was opened to traffic until the date of data collection. Both directions are taken into account. The exact dates of both the road opening (or the most recent M&R activity) and data collection activities were used for its calculation.
- **Total Heavy Vehicles (TotalHVeh):** the total number of heavy vehicles circulating in both directions on the segment of road since its opening or since the most recent M&R activity up until the date of IRI data collection, and expressed in millions of heavy vehicles. The precise dates of the road opening and data collection activities were used for its calculation.
- **Total thickness of bituminous layers (BitThick):** a standard variable employed in roughness modelling [19, 88, 101, 105], which was therefore incorporated in the analysis. It represents the total thickness of the bituminous layers (surface, base, and subbase layers) in the pavement section, expressed in cm., considering all of the bituminous layers.
- **Environmental data:** as previously commented, climatic conditions within Gipuzkoa are quite similar, so there are no observable differences due to weathering throughout the road network. For example, annual average precipitation ranges between 1300 and 2000 mm within the province and between 1400 and 1600 mm within the areas of the selected freeways. Such a small difference was therefore not considered to be a real affecting factor. Consequently, environmental data were not considered to be a significant influencing factor.
- **Pavement type (PaveType):** a qualitative, non-numerical variable, which refers to pavement type: flexible, semi-rigid or composite. There are no rigid pavements in Gipuzkoa.
- **International Roughness Index (IRI):** the dependent variable that is to be predicted. As mentioned above, the PCG conducts an assessment of road network conditions based on data collection, and roughness values are indicated using the IRI. However, the IRI was only recorded throughout the entire road network in 2018 and 2021. IRI

values are specified for every 100 metres of the road, indicating the exact initial and final Kilometre Points (KPs) of each segment, considering each carriageway separately on double carriageway roads. IRI values for the right-hand lane were recorded for each carriageway. The IRI is measured in the right-hand lane where deterioration is higher due to higher rates of heavy vehicle circulation. IRI data were recorded for the left and the right wheel paths of the right-hand lane, which therefore yielded two IRI values. The mean value of both could be calculated, although it was decided to maintain both values with the aim of reflecting a degree of variability in the values. When analysing the IRI values for each 100-metre section, wide variance was observed within sections with the same predictive values. For example, in a homogeneous 2 km stretch with the same pavement section from the same project and traffic volume, the 20 IRI values of each wheel path (left and right wheel paths, considered separately) showed variance. Therefore, the mean IRI was calculated for both wheel paths (right and left) on each stretch with identical pavement structure characteristics in age and traffic volume. It is a logical and common approach [88, 101], as deterministic models are meant to predict the mean IRI from certain variables, unlike probabilistic models for which the complete range of values is considered [70].

There were no further PMS database variables for inclusion in the modelling process. With these variables or transformed variables, firstly an MLR was developed, using all the numerical variables (excluding PaveType). Then, a GLM was created using all the (quantitative and qualitative) variables, as shown in Figure 1.

4. Results and Discussion

4.1. Multiple Linear Regression Model

After segmenting sections of the dual carriageway road network of Gipuzkoa with similar pavement structure characteristics, ages and traffic volumes, including flexible, semi-rigid, and composite pavements, a dataset of 119 stretches was compiled for modelling purposes. The dependent variable in this analysis was the average IRI over the selected sections, while potential predictor (independent) variables included Age, RealAge, BitThick, AADT, AADT-HV, AADTprev, AADT-HVprev, TotalVeh, and TotalHVeh.

First, the correlations between each of the nine independent variables and the IRI were calculated using the Pearson correlation coefficient (R), and the significance of the correlations was then analysed (Table 1).

Table 1. Correlations between IRI and the independent variables (Pearson coefficient, R) and significance of the correlations

Independent Variables	Correlation with IRI (Pearson coefficient, R)	Significance of the Correlation (Bilateral)
Age	0.342**	< 0.001
RealAge	0.349**	< 0.001
BitThick	0.478**	< 0.001
AADT	-0.020	0.832
AADT-HV	0.053	0.568
AADTprev	0.020	0.827
AADT-HVprev	0.058	0.533
TotalVeh	0.497**	< 0.001
TotalHVeh	0.557**	< 0.001

** Significance level of correlation 0.01.

The analysis of the correlations between the dependent variable and the various independent variables revealed some remarkable results. On the one hand, the strongest correlations were observed with the following variables: TotalHVeh, TotalVeh, BitThick, RealAge, and Age. On the other hand, variables such as AADT, AADT-HV, AADTprev, and AADT-HVprev yielded low correlations that were not statistically significant. It can be logically construed that high annual traffic volumes over a freshly laid pavement (only a few years old) will not deteriorate as much as an old pavement with lower annual traffic volumes [26].

Additionally, transformations of the variables were explored, so that the curves that best captured the relations between the dependent variable and each independent variable could be obtained. Table 2 shows the equations that generated the curves that yielded optimal fits. Nonetheless, the curves that showed superior fits were not always selected, since the quadratic and the cubic curves produced better fits, even though they never represented an expected pattern proposed in the literature, which in no case simulated experimental patterns [101]. Furthermore, in cases where the marginal improvement in the coefficient of determination (ΔR^2) from linear to other curves was negligible ($\Delta R^2 < 0.05$), the linear model was retained and the predicting variable was not transformed.

Table 2. Best correlations of each individual independent variable with the dependent variable

Independent Variable	Equation Type	R ²	Summary of the Model				Parameter Estimates		
			F	Sig.	Degrees of freedom 1	Degrees of freedom 2	Intercept	b1	b2
Age	Quadratic	0.213	15.656	<0.001	2	116	1.690	-0.066	0.010
RealAge	Quadratic	0.226	16.911	<0.001	2	116	1.717	0.071	0.010
BitThick	Lineal	0.229	34.676	<0.001	1	117	0.788	0.046	
AADT	Inverse	0.015	1.796	0.183	1	117	1.564	3048.76	
AADT-HV	Quadratic	0.019	1.110	0.333	2	116	1.433	4.95·10 ⁻⁶	1.02·10 ⁻⁷
AADTprev	Quadratic	0.022	1.28	0.282	2	116	1.187	5.46·10 ⁻⁵	9.91·10 ⁻¹⁰
AADT-HVprev	Potential	0.033	4.033	0.047	1	117	1.004	0.070	
TotalVeh	Quadratic	0.274	21.907	<0.001	2	116	1.459	-0.01	5.620·10 ⁻⁵
TotalHVeh	Quadratic	0.331	28.682	<0.001	2	116	1.440	0.004	0.007

As shown, various modifications can be implemented to improve the correlation between each predictor variable and the IRI (the dependent variable). Age and RealAge improved their correlation using a quadratic transformation (Age² and RealAge²), but BitThick showed a better correlation with a linear relationship. Once again, RealAge showed a better correlation than Age. In the case of annual traffic volumes, there was no improvement with their correlations with IRI, and no significant models were obtained (except for the case of AADT-HVprev).

Utilising transformed and untransformed variables, the influence of each factor was assessed in a multiple linear regression framework using step-by-step and forward functions. The MLR models were built and tested using SPSS Statistics software v. 28. Furthermore, if different MLR models showed global significance (if a p-value lower than 0.05 was obtained in the Fisher-Snedecor test) and if all the variables were of significance (in Student *t*-tests), then they were explored and accepted. Table 3 presents a subset of the tested models.

Table 3. Proposed MLR for IRI performance in flexible, semi-rigid and composite pavements in Gipuzkoa

Proposed Model	R ²	Comments and Observations
IRI= Int + BitThick + TotalHVeh ² + TotalVeh ²	0.451	Medium significance of TotalVeh ² (p = 0.09)
IRI= Int + BitThick + Age ² + TotalVeh ²	0.645	All variables are significant (p < 0.05)
IRI= Int + BitThick + RealAge ² + TotalVeh ²	0.649	All variables are significant (p < 0.05)
IRI= Int + BitThick + RealAge ² + TotalVeh + TotalVeh ²	0.650	No significance of TotalVeh (p = 0.569)
IRI= Int + RealAge + TotalHVeh ² + TotalVeh ²	0.557	Low significance of TotalVeh ² (p = 0.064)
IRI= Int + Age ² + TotalHVeh ² + TotalVeh ²	0.672	All variables are significant (p < 0.05)
IRI= Int + RealAge ² + TotalHVeh ² + TotalVeh ²	0.679	All variables are significant (p < 0.05)
IRI= Int + BitThick + RealAge ² + TotalHVeh + TotalH Veh ²	0.700	Low significance of TotalHVeh (p = 0.195)
IRI= Int + BitThick + RealAge ² + TotalVeh + TotalHVeh ²	0.701	Low significance of TotalVeh (p = 0.165)
IRI= Int + BitThick + Age ² + TotalHVeh ²	0.696	All variables are significant (p < 0.05)
IRI= Int + BitThick + RealAge ² + TotalHVeh ²	0.696	All variables are significant (p < 0.05)
IRI= Int + BitThick + RealAge ² + TotalHVeh ² + TotalVeh ²	0.713	All variables are significant (p < 0.05)

The summary of tested models in Table 3 shows that the variables BitThick, RealAge², and TotalHVeh² were always significant in the different models that were tested. Additionally, RealAge² provided higher accuracy than Age², highlighting the importance of knowing the exact age and introducing the precise dates of both construction (or M&R activities) and data collection [26]. The last two models on the list had the highest coefficients of determination, all the variables of which were significant. The last one, with a higher R² (0.713), had some problems in the collinearity diagnosis. In particular, one Correlation Index was 16.843 and the Variance Inflation Factor of both TotalVeh² and TotalHVeh² was over 23, exceeding the usual limit of 10 for not considering multicollinearity. In fact, both variables were highly correlated, with a Pearson coefficient (R) of 0.974. This extremely high value was due to the small variance of the percentage of heavy vehicles in Gipuzkoa, which is between 3 and 10%. Consequently, it was preferred to propose the preceding model, of almost similar accuracy (R² = 0.696), and to verify all the hypotheses of an MLR model, as shown in in Equation 9:

$$IRI = 0.772 + 0.020 \cdot TotBit + 0.007 \cdot RealAge^2 + 0.008 \cdot TotHVeh^2 \quad (9)$$

where IRI is the predicted mean IRI (m/km) value of the segment with identical variable values of age, traffic, and thickness of bituminous layers in flexible, semi-rigid, and composite pavements. RealAge is the actual age of the pavement, computed from the precise date of the road opening (or the most recent M&R activity) up until the desired evaluation time, expressed as a decimal fraction. BitThick is the total thickness of the bituminous layers over flexible, semi-rigid, and composite pavements, measured in centimetres. TotalHVeh is the cumulative number of heavy vehicles that have traversed the segment during the specified period, since the road was opened to traffic (or the most recent M&R activities) up until the desired evaluation time, expressed per million of heavy vehicles.

The statistical results of the model described in Equation 9 are presented in Tables 4 to 6 and Figure 2. Examination of the model parameters in Table 4 revealed a highly significant F-test result with a p-value < 0.001, confirming the validity of the proposed relations. In addition, the parameter coefficients were found to be significant and different from zero based on Student t-tests, as evidenced by the 95% confidence intervals not including zero. The significance of the model is the first point to be checked in any MLR.

Table 4. Analysis of Variance of the Equation 9 based Model and Parameter Estimates

Source	Sum of Squares	d.o.f.	Mean Squares	F value	p-Value	Durbin-Watson	Root Mean Square Error	R
Model	35.772	3	11.924					0.834
Error	15.640	115	0.136	87.676	<0.001	1.075	R ²	Adj. R ²
Corrected total	51.412	118					0.696	0.688

Parameter Estimates							Collinearity Statistics	
Variable	Parameter Estimate	Std. Error	t Value	p-Value	Lower bound	Upper bound	Tolerance	VIF
Intercept	0.772	0.108	7.119	<0.001	0.557	0.987		
BitThick	0.020	0.005	3.590	<0.001	0.009	0.030	0.841	1.188
RealAge ²	0.007	0.001	10.263	<0.001	0.005	0.008	0.923	1.083
TotalHVeh ²	0.008	0.001	10.787	<0.001	0.007	0.009	0.818	1.223

Table 5. Coefficient correlation, R, between the independent variables of the model based on Equation 9

		TotalHVeh ²	RealAge ²	BitThick
Correlations	TotalHVeh ²	1.000	0.256	-0.385
	RealAge ²	0.256	1.000	-0.196
	BitThick	-0.385	-0.196	1.000
Covariances	TotalHVeh ²	5.528·10 ⁻⁷	1.263·10 ⁻⁷	-1.560·10 ⁻⁶
	RealAge ²	1.263·10 ⁻⁷	4.406·10 ⁻⁷	-7.082·10 ⁻⁷
	BitThick	-1.560·10 ⁻⁶	-7.082·10 ⁻⁷	2.965·10 ⁻⁵

Table 6. Collinearity diagnosis of Equation 9

Dimension	Eigenvalue	Condition Index	Proportions of the variance			
			Intercept	BitThick	RealAge ²	TotalHVeh ²
1	2.854	1.000	0.01	0.01	0.04	0.03
2	0.781	1.912	<0.01	<0.01	0.46	0.27
3	0.317	2.999	0.07	0.03	0.50	0.62
4	0.047	7.759	0.92	0.96	0.01	0.08

The evaluation of the Durbin-Watson statistic yielded a value of 1.249, confirming the independence of the errors and the absence of autocorrelation (Table 4). Furthermore, the analysis revealed no significant correlations between the independent variables of the model, with a low-medium Pearson coefficient (R = -0.385) between BitThick and TotalHVeh² (Table 5). Besides, the Variance Inflation Factors of all the variables were low (VIF < 10) (Table 6). No patterns of homoscedasticity were visually discernible in Figure 2. No Correlation Index exceeded 30 (Table 6), suggesting that there were no multicollinearity problems and therefore an absence of multicollinearity. The residual analysis showed that the distribution was normal, verified by the Shapiro-Wilk test. Additionally, the plot of observed values versus predicted values of the model shown in Figure 3 is closely aligned with the main diagonal, indicating a satisfactory fit of the model.

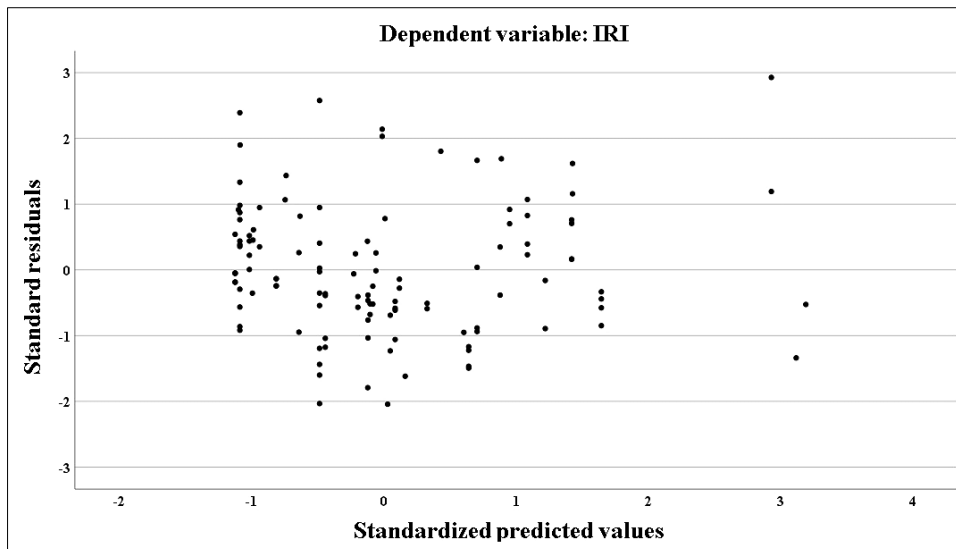


Figure 2. Scatter plot of the standardized predicted values vs. standardized residuals of Equation 9

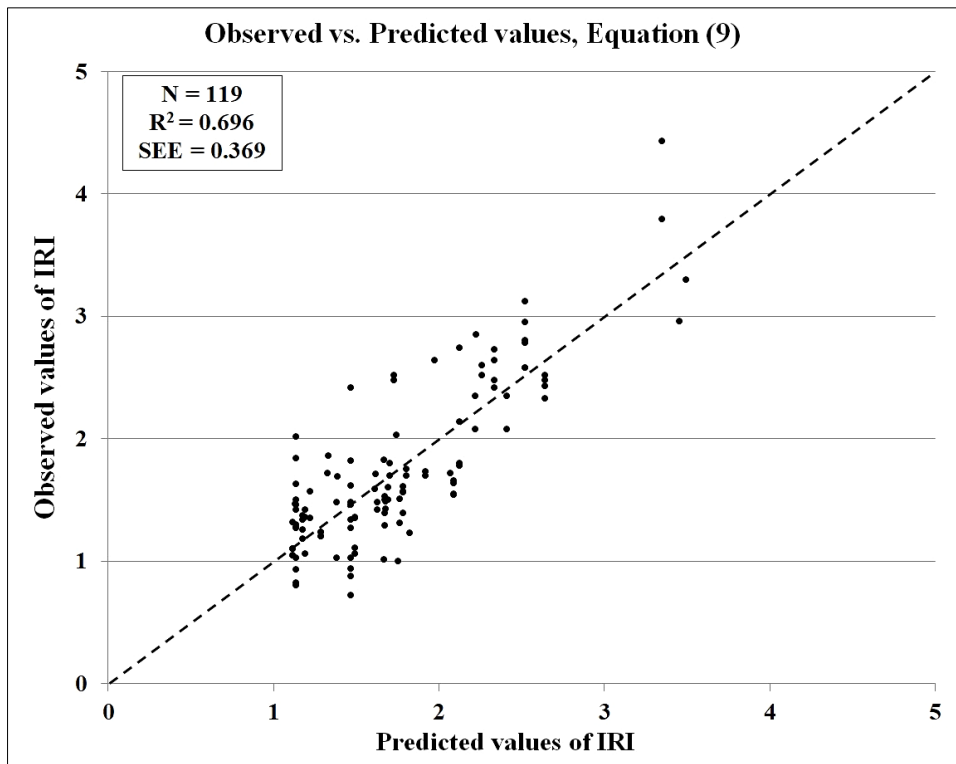


Figure 3. Observed values vs. Predicted values of Equation 9

The selected variables had a significant impact on the evolution of the IRI. Moreover, the exact influence of each factor can be easily inferred with the deterministic approach that was selected [87, 88]. Specifically, an increase in real age and accumulated heavy vehicles was associated with higher IRI values. Additionally, the exact age of the pavement, rather than solely time elapsed since construction, was considered critical for accurate modelling. Positive correlations between IRI and the variables traffic and age have been widely verified in the literature [108, 117, 118]. The coefficient of BitThick indicated that thicker bituminous layers implied greater deterioration (expressed by the IRI), which could be contradictory. Higher bituminous layer thicknesses have always been correlated with more resistant pavements [19, 117]. However, when heavy traffic is expected on a motorway, stronger structural solutions are chosen, with semi-rigid being preferred to flexible pavements thanks to their greater load-bearing capacity. It should at this point be mentioned that semi-rigid pavements are generally designed with thinner bituminous layers due to the higher compressive strength and modulus of elasticity of the treated materials of the base and subbase layers [101, 119]. As shown, all the coefficients in Equation 9 are logical and reflect the influence on IRI progression, as well as being highly significant.

4.2. Generalized Linear Model (GLM) Including a Qualitative Variable

While Equation 9 incorporated the bituminous layer thickness effect, different pavement materials and their potential influence were overlooked to achieve a single equation applicable to all pavement types. Nevertheless, it is plausible to infer that, in addition to layer thickness, different base materials may have a significant role in IRI progression. Indeed, as mentioned in the introduction, flexible, semi-rigid, and composite pavements all performed in different ways due to the specific compressive resistance of each base material [19, 92, 93, 101, 102, 104]. Therefore, a qualitative variable called *PaveType* was introduced in the model so as to account for the base materials and their different effects on the evolution of the IRI. Considering the base material, this variable was used to categorise pavement structures into flexible pavements (32 sections), semi-rigid pavements (71), and composite pavements (16).

A GLM was employed due to the inclusion of a qualitative variable. Several models were then tested by combining the available quantitative variables (those from the previous model) with the qualitative variable, *PaveType*. The aim was only to include the significant variables, i.e., those that really influenced the progression of the IRI. Table 7 shows some of the numerous trials that were examined, listing those of higher accuracy.

Table 7. Proposed GLM models for IRI performance in flexible, semi-rigid, and composite pavements in Gipuzkoa

No.	Proposed Model	R ²	Comments and Observations
1	IRI= Int + BitThick + RealAge ² + TotalHVeh ² + PaveType	0.781	All variables are significant (p < 0.05)
2	IRI= Int + BitThick + RealAge ² + TotalHVeh ² + TotalVeh ² + PaveType	0.781	TotalVeh is not significant (p = 0.963)
3	IRI= Int + BitThick + RealAge + TotalHVeh ² + PaveType	0.713	All variables are significant (p < 0.05)
4	IRI= Int + BitThick + RealAge ² + TotalVeh ² + PaveType	0.777	All variables are significant (p < 0.05)
5	IRI= Int + BitThick + RealAge + TotalVeh ² + PaveType	0.716	All variables are significant (p < 0.05)
6	IRI= Int + PaveType* BitThick + RealAge + TotalHVeh	0.697	All variables are significant (p < 0.05)
7	IRI= Int + PaveType* BitThick + RealAge + TotalHVeh + TotalVeh	0.698	TotalVeh (p = 0.588) and TotalHVeh (p = 0.331) are not significant
8	IRI= Int + PaveType* BitThick + RealAge + TotalHVeh ²	0.708	All variables are significant (p < 0.05)
9	IRI= Int + BitThick + PaveType* RealAge ² + TotalHVeh ² + TotalVeh ²	0.750	No significance of BitThick (p = 0.918)
10	IRI= Int + PaveType* BitThick + RealAge ² + TotalVeh	0.753	All variables are significant (p < 0.05)
11	IRI= Int + BitThick + PaveType*RealAge + TotalHVeh ²	0.675	No significance of BitThick (p = 0.155)
12	IRI= Int + PaveType*BitThick + RealAge ² + TotalVeh ²	0.763	All variables are significant (p < 0.05)
13	IRI= Int + PaveType*BitThick + RealAge ² + TotalHVeh	0.769	All variables are significant (p < 0.05)
14	IRI= Int + PaveType*BitThick + RealAge ² + TotalHVeh ²	0.773	All variables are significant (p < 0.05)
15	IRI= Int + PaveType*BitThick + RealAge ² + TotalHVeh + TotalVeh	0.770	No significance of TotalVeh (p = 0.466)
16	IRI= Int + PaveType*BitThick + RealAge ² + TotalHVeh + TotalVeh ²	0.771	No significance of TotalVeh ² (p = 0.322)
17	IRI= Int + PaveType*BitThick + RealAge ² + TotalHVeh ² + TotalVeh	0.773	No significance of TotalVeh (p = 0.692)
18	IRI= Int + PaveType*BitThick + RealAge ² + TotalHVeh ² + TotalVeh ²	0.773	No significance of TotalVeh ² (p = 0.618)
19	IRI= Int + PaveType*BitThick + RealAge ² + PaveType*TotalHVeh ²	0.774	All variables are significant (p < 0.05)
20	IRI= Int + PaveType*BitThick + RealAge ² + PaveType*TotalHVeh ² + TotalVeh ²	0.775	No significance of TotalVeh ² (p = 0.438), medium significance of PavType*TotalH.Veh ² (p = 0.115)
21	IRI= Int + PaveType*BitThick + PaveType*RealAge + TotalHVeh ²	0.776	All variables are significant (p < 0.05)
22	IRI= Int + PaveType*BitThick + PaveType*RealAge ² + TotalHVeh ²	0.788	All variables are significant (p < 0.05)
23	IRI= Int + PaveType*BitThick + PaveType* RealAge ² + TotalHVeh ² + TotalVeh ²	0.789	No significance of TotalVeh ² (p = 0.488)
24	IRI= Int + PaveType*BitThick + PaveType*RealAge ² + PaveType*TotalHVeh ²	0.790	All variables are significant (p < 0.05)
25	IRI= Int + PaveType*BitThick + RealAge ² + TotalHVeh ² + PaveType	0.786	All variables are significant (p < 0.05)
26	IRI= Int + BitThick + PaveType*RealAge ² + TotalHVeh ² + PaveType	0.795	All variables are significant (p < 0.05)
27	IRI= Int + PaveType*BitThick + PaveType*RealAge ² + TotalHVeh ² + PaveType	0.800	All variables are significant (p < 0.05)
28	IRI= Int + PaveType*BitThick + PaveType*RealAge ² + PaveType*TotalHVeh ² + PaveType	0.808	All variables are significant (p < 0.05)

In Table 7, the summary of the models that were tested merits some reflection. If only one of the variables, TotalVeh² or TotalHVeh², was included, then the model was significant when the qualitative variable was introduced even though it was not combined with any quantitative variables (models 1-5). As with the MLR models, RealAge² achieved a better R² than RealAge. When PaveType was combined with the quantitative variables, all the variables of the models were

significant including the combination *PaveType***BitThick*, (models 6, 8, 10, and 12-14), given that only one traffic variable was included. Models with both traffic volume variables showed non-significant variables (model 7, 15-18, 20 and 23). A result that underlines the strong correlation between the two variables, as commented in the MRL section. It can be concluded that the pavement type is directly related to the bituminous thickness, as shown in the pavement design guides [84, 85, 100, 111]. However, when *PaveType* was only combined with *RealAge* (*PaveType***RealAge*), *BitThick* became insignificant (models 9 and 11 of Table 7). Finally, the qualitative variable can be combined with two quantitative variables, obtaining a higher determination coefficient (R^2) (models 19, 21, and 22) and even higher when combined with three quantitative variables (model 24), as long as *TotalVeh* and *TotalHVeh* were not included together. Additionally, good results were obtained when *PaveType* was introduced as a separate variable and combined with quantitative variables (models 25-28).

The choice of the proposed model, in which all the variables were significant, was between the best solutions for each type of model that was developed:

- Without combining the qualitative variables with the quantitative ones (model 1);
- Combined with one, *BitThick* (model 14);
- Combined with two quantitative variables (model 22);
- Combined with three (model 24);
- Separately included and combined with other quantitative variables (models 25-28).

The coefficient of determination was at that point yet to be employed as a unique index for model selection. In general, models with more variables obtained higher accuracy levels (R^2) (as long as all the variables were significant). However, the adjusted R^2 (*Adj. R²*) index takes into account the obtained R^2 and the number of variables used. The adjusted factors of the preselected models are presented in Table 8. Furthermore, in addition to the fact that all the variables were significant, the model shown in Table 8 was preferred, in which all the coefficients of each variable were also significant.

Table 8. Adjusted R^2 and significance of all the coefficients of the pre-selected models for GLM

No.	Proposed Model	R^2	Adj. R^2	Comments and Observations
1	$IRI = Int + BitThick + RealAge^2 + TotalHVeh^2 + PaveType$	0.781	0.771	All coefficients significant ($p < 0.001$)
14	$IRI = Int + PaveType * BitThick + RealAge^2 + TotalHVeh^2$	0.773	0.763	All coefficients significant ($p < 0.012$)
22	$IRI = Int + PaveType * BitThick + PaveType * RealAge^2 + TotalHVeh^2$	0.788	0.775	All coefficients significant ($p < 0.041$)
24	$IRI = Int + PaveType * BitThick + PaveType * RealAge^2 + PaveType * TotalHVeh^2$	0.790	0.772	The coefficient of [<i>PaveType</i> =Composite]* <i>TotalHVeh</i> ² is not significant ($p = 0.936$)
25	$IRI = Int + PaveType * BitThick + RealAge^2 + TotalHVeh^2 + PaveType$	0.786	0.775	The coefficient of <i>PaveType</i> =Semi-rigid]* <i>BitThick</i> is not significant ($p = 0.815$)
26	$IRI = Int + BitThick + PaveType * RealAge^2 + TotalHVeh^2 + PaveType$	0.795	0.782	All coefficients significant ($p < 0.038$)
27	$IRI = Int + PaveType * BitThick + PaveType * RealAge^2 + TotalHVeh^2 + PaveType$	0.800	0.785	Two coefficients not significant ($p > 0.275$)
28	$IRI = Int + PaveType * BitThick + PaveType * RealAge^2 + PaveType * TotalHVeh^2 + PaveType$	0.808	0.790	Three coefficients not significant ($p > 0.164$)

As shown in Table 8, models 24, 25, 27, and 28 were rejected because at least one of the coefficients was not significant. Among the remaining models (models 1, 14, 22, and 26), model 26 had a higher R^2 (0.795) and a higher adjusted R^2 (0.782). Finally, both model 1 and model 26 (Table 8) were proposed. Model 1 was chosen because of its simplicity. The qualitative variables were directly introduced into the model with no need to combine them, and the same variables that appear in Equation 9 were used. Model 1 is shown in Equation 10:

$$IRI = 1.904 - 0.038 \cdot TotBit + 0.007 \cdot RealAge^2 + 0.006 \cdot TotHVeh^2 + PaveType \tag{10}$$

where *BitThick*, *RealAge*, and *TotalHVeh* are defined in Equation 9 and *PaveType* is a variable that takes into account the pavement type according to the base material and takes the values listed in Table 9:

Table 9. Values of the variable *PaveType* in Equation 10

Pavement Type	Base Material	PaveType
Flexible pavement	Granular material	0.807
Semi-rigid pavement	Treated material	0
Composite pavement	Concrete	-0.739

Model 26 is presented in Equation 11:

$$IRI = 2.054 - 0.042 \cdot TotBit + A \cdot RealAge^2 + 0.006 \cdot TotHVeh^2 + PaveType \tag{11}$$

where BitThick, RealAge, and TotalHVeh are defined in Equation 9, A and PaveType are coefficients that take into account the pavement type based on the base material, with the values given in Table 10.

Table 10. Values of the variables A and PaveType in Equation 11

Pavement Type	Base Material	A	PaveType
Flexible pavement	Granular material	0.008	0.709
Semi-rigid pavement	Treated material	0.005	0
Composite pavement	Concrete	0.004	-0.664

The model based on Equation 10 was statistically analysed, as shown in Tables 11 and 12 and Figures 4 to 5. The new model, including the pavement type, improved its predictive accuracy, with a coefficient of determination ($R^2 = 0.781$) that was higher than the previous model (Equation 9). The test of the Between-Subjects effect of Equation 1 is presented in Table 11, in which all the variables had a very high significance, with a p-value lower than 0.001. Furthermore, Table 12 presents the coefficients of the model, i.e., the estimates of the parameters, which again show a very high significance (p-values < 0.001). No coefficient was therefore zero with a confidence level higher than 99.99%. The extremely high significance levels of all the coefficients clearly demonstrate the adequacy of the selected variables for modelling, reflecting their importance in the IRI evolution. The dispersion graph of the variance by level in Figure 3 shows that the points are not horizontally aligned, meaning non-homogeneous variances between the levels of PaveType, which is a key characteristic that must be verified in GLM regression equations [21]. The plot of predicted values against the standardised residuals in Figure 5 was random (no patterns observed), so the residuals showed no interdependence. This point must also be checked in a GLM equation. Besides, in Figure 6, the observed and the predicted IRI values were close to the main diagonal, highlighting the high accuracy of the model.

Table 11. Test of Between-Subjects effects of the model based on Equation 10

Origin	Type III sum of squares	d.o.f.	Mean Square	F	Sig.	Non-Centrality Parameter
Corrected model1	40.129	5	8.026	80.379	< 0.001	401.895
Intercept	9.451	1	9.451	94.650	< 0.001	94.650
BitThick	1.433	1	1.433	14.350	< 0.001	14.350
RealAge2	14.839	1	14.839	148.617	< 0.001	148.617
TotalHVeh2	5.971	1	5.971	59.796	< 0.001	59.796
PaveType	4.357	2	2.179	21.818	< 0.001	43.636
Error	11.283	113	0.100			
Total	410.248	119				
Corrected total	51.412	119				

$R^2 = 0.781$ (adjusted $R^2 = 0.771$).

Table 12. Parameter estimates for the model based on Equation 10

Parameter	B	Std. Error	t	Sig.	95% CI		Non-Centrality Parameter	Observed Power
					Lower bound	Upper bound		
Intercept	1.904	0.201	9.476	< 0.001	1.506	2.302	9.476	1.000
BitThick	-0.038	0.010	-3.788	< 0.001	-0.058	-0.018	3.788	0.964
RealAge ²	0.007	0.001	12.191	< 0.001	0.006	0.009	12.191	1.000
TotalH.Veh ²	0.006	0.001	7.733	< 0.001	0.004	0.007	7.733	1.000
[PaveType =Flexible]	0.807	0.127	6.342	< 0.001	0.555	1.059	6.342	1.000
[PaveType = Composite]	-0.739	0.145	-5.082	< 0.001	-1.028	-0.451	5.082	0.999
[PaveType = Semi-rigid]	0 ^a							

^a Set to zero because this parameter is redundant.

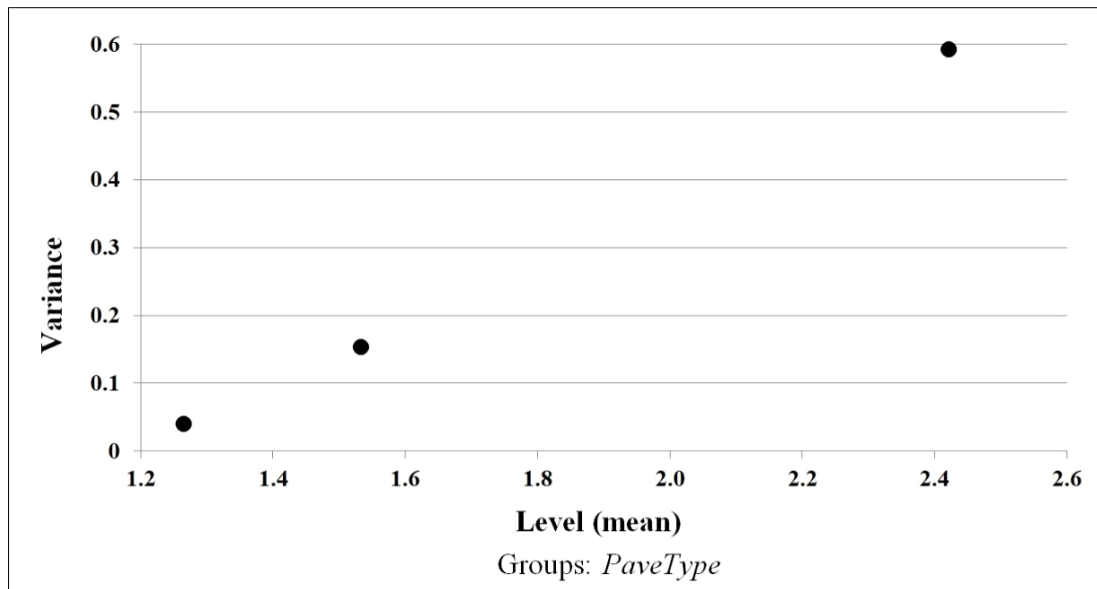


Figure 4. Scatter plots of the variance by level for Equation 10

Dependent variable: IRI

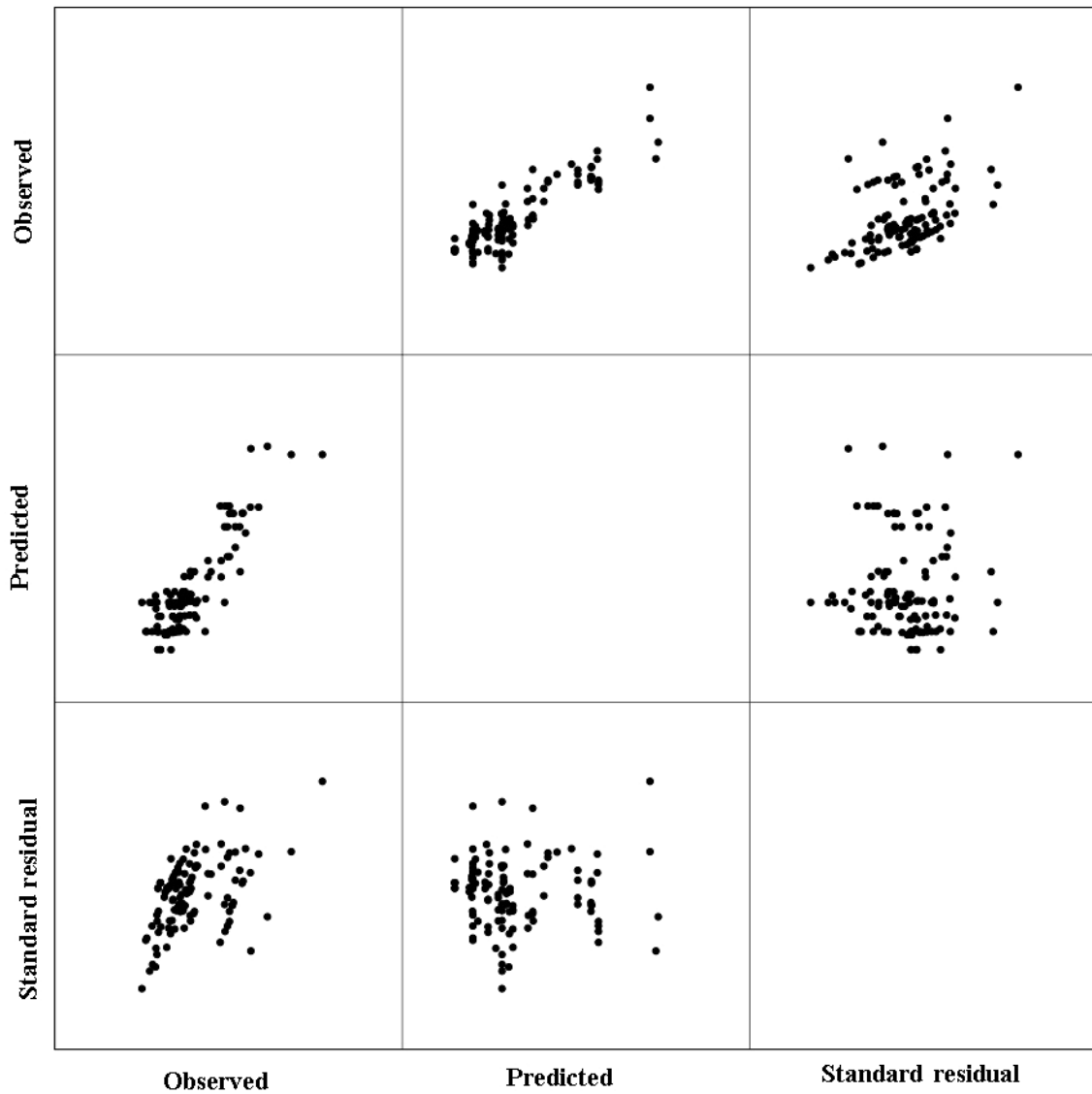


Figure 5. Plot of residuals (standardized), observed and predicted values of the model based on Equation 10

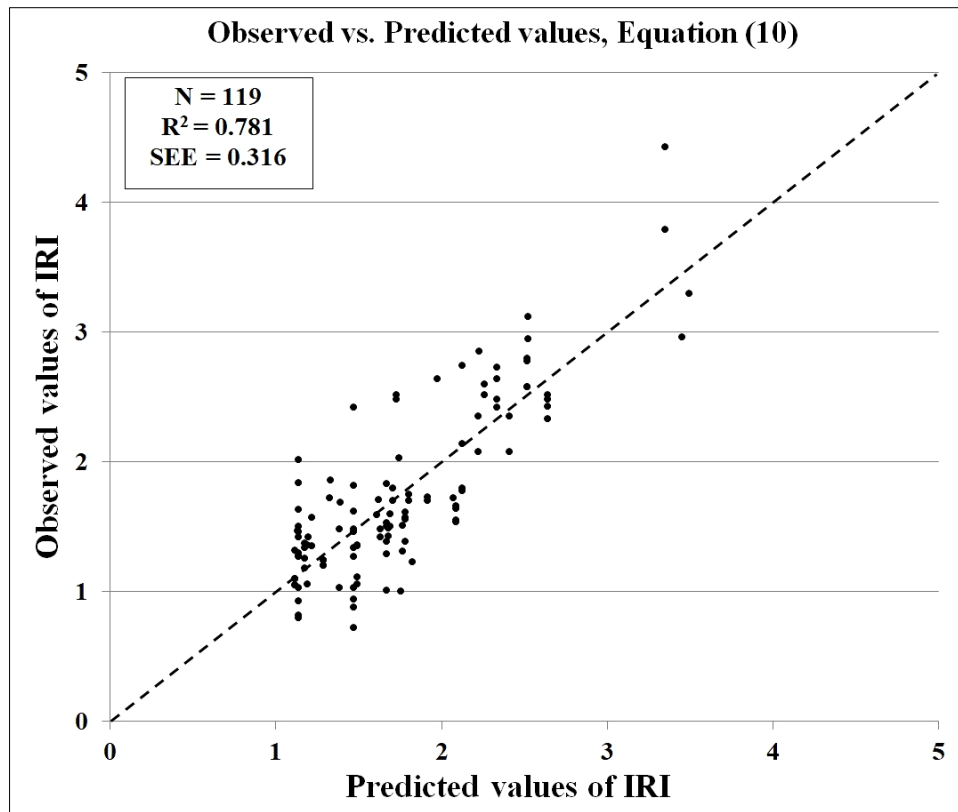


Figure 6. Observed values vs. Predicted values with Equation 10

Tables 13 and 14 and Figures 7 to 9 show the statistical analysis of the model based on Equation 11.

Table 13. Test of Between-Subjects effects of the model based on Equation 11

Origin	Type III sum of squares	d.o.f.	Mean Square	F	Sig.	Non-Centrality Parameter	Observed Power
Corrected model1	40.862	7	5.837	61.422	< 0.001	429.952	1.000
Intercept	10.068	1	10.068	105.931	< 0.001	105.931	1.000
BitThick	1.726	1	1.726	18.159	< 0.001	18.159	0.988
PaveType*RealAge ²	15.573	3	5.191	54.619	< 0.001	163.856	1.000
TotalHVeh ²	6.467	1	6.467	68.042	< 0.001	68.042	1.000
PaveType	3.117	2	1.558	16.397	< 0.001	32.794	1.000
Error	10.549	111	0.095				
Total	410.248	119					
Corrected total	51.412	118					

R² = 0.795 (adjusted R² = 0.782)

Table 14. Parameter estimates for the model based on Equation 11

Parameter	B	Std. Error	t	Sig.	95% CI		Non-Centrality Parameter	Observed Power
					Lower bound	Upper bound		
Intercept	2.054	0.205	10.005	< 0.001	1.647	2.461	10.005	1.000
BitThick	-0.042	0.01	-4.261	< 0.001	-0.062	-0.023	4.261	0.988
[PaveType=Flexible]*RealAge ²	0.008	0.001	12.174	< 0.001	0.007	0.010	12.174	1.000
[PaveType=Semi-rigid]*RealAge ²	0.005	0.001	3.082	0.003	0.002	0.007	3.082	0.863
[PaveType=Mixed]*RealAge ²	0.004	0.002	2.102	0.038	0.0002	0.008	2.102	0.549
TotalHVeh ²	0.006	0.001	8.249	< 0.001	0.005	0.007	8.249	1.000
[PaveType=Flexible]	0.709	0.132	5.372	< 0.001	0.447	0.970	5.372	1.000
[PaveType=Semi-rigid]	0 ^a							
[PaveType=Mixed]	-0.664	0.189	-3.514	< 0.001	-1.038	-0.289	3.514	0.936

^a Set to zero because this parameter is redundant

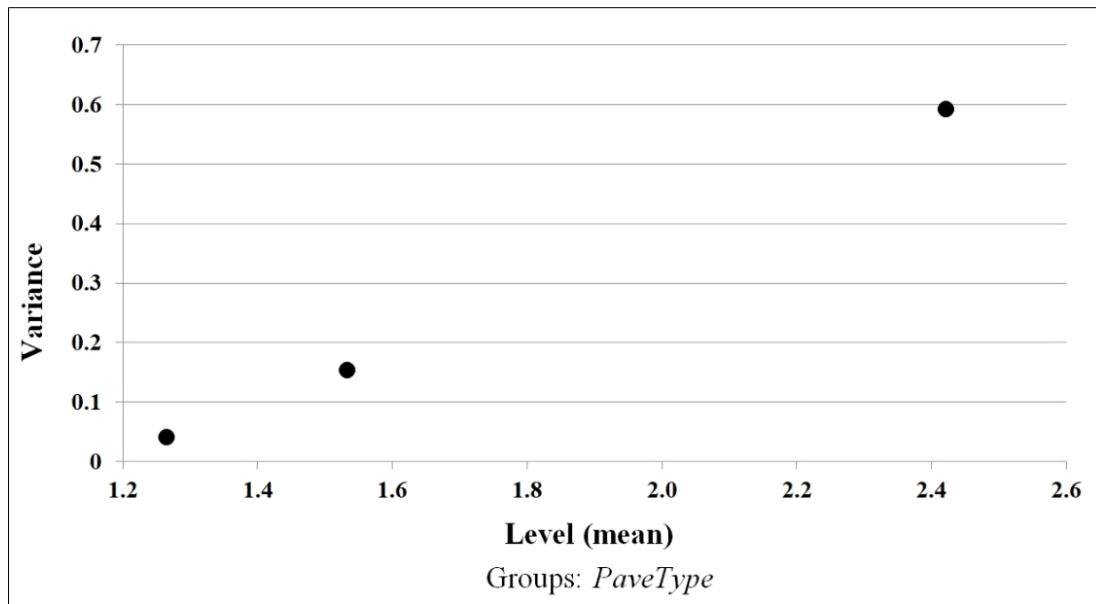


Figure 7. Scatter plots by level of variance for Equation 11

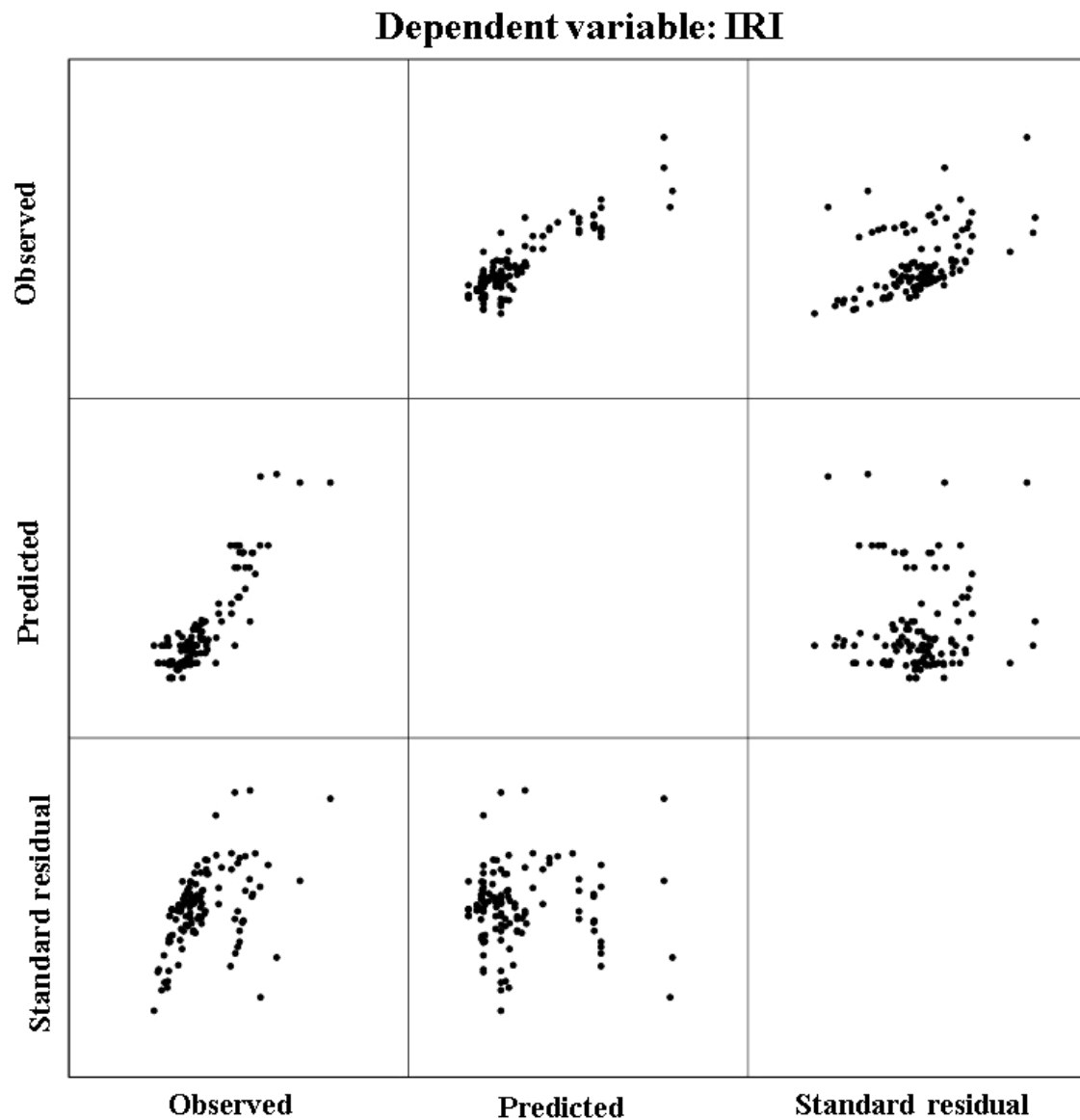


Figure 8. Plot of observed (standardized) residuals, and predicted values of the model based on Equation 11

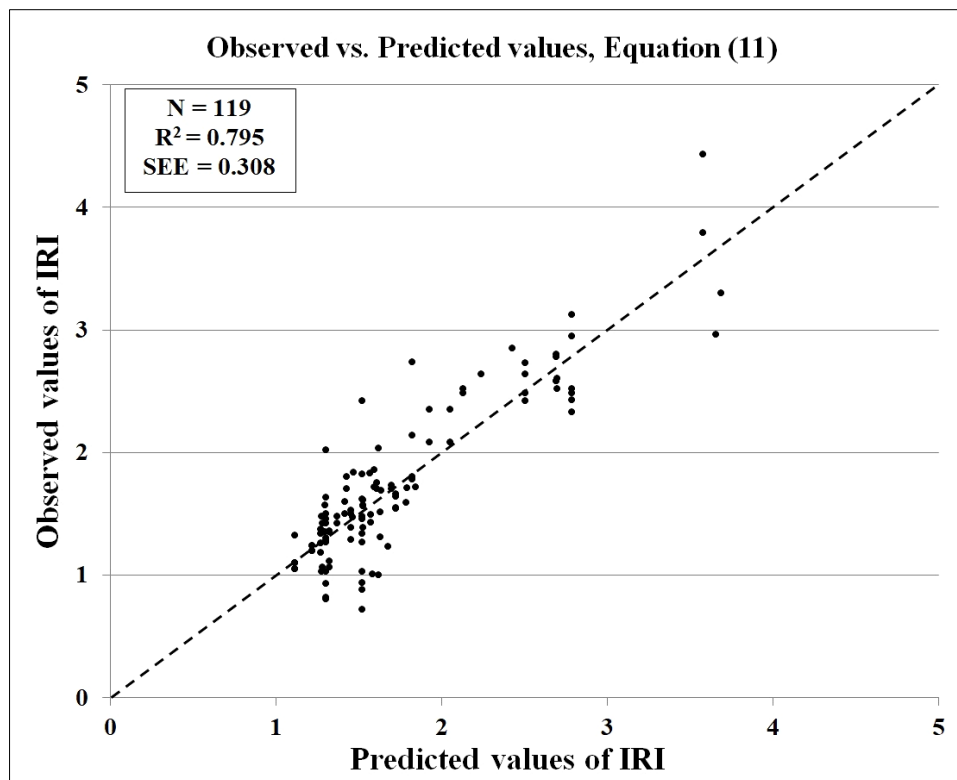


Figure 9. Observed values vs. Predicted values with Equation 11

Table 13 presents the Between-Subject effects test for the model based on Equation 11, with all the variables showing high levels of significance, as indicated by their respective p-values all below 0.001. Moreover, the individual significance of each parameter (Table 14) was also considerable, with the highest p-value at 0.038. It indicated that not all the coefficients were equal to zero with a 96.2% confidence level. Once again, these high significances confirmed that the right variables had been chosen for accurate modelling of pavement deterioration. Figure 7 illustrates the dispersion diagrams by level, offering a visual representation of the variance homogeneity. The absence of horizontal alignment between the points in Figure 7 means that the variances are not equal. There was therefore no identifiable relationship between the respective sizes of the means and the variance. It can be observed in Figure 8 that the plot of predicted values versus standardised results was random, lacking any discernible pattern. Additionally, the errors were homogeneous, as evidenced by the similar dispersion of the standardised residuals across all predicted values. Figure 9 depicts a plot of predicted values versus observed values, with all the points situated close to the main diagonal, reflecting the high accuracy of the presented model.

The proposed models (Equations 10 and 11) serve to reinforce the idea that the pavement type, whether flexible, semi-rigid or mixed, is a fundamental variable for the creation of a global pavement performance prediction model. The disparate behaviour of the models under traffic loads is reflected in the enhanced accuracy of both models, with R^2 values of 0.781 and 0.795, in comparison with the model without *PaveType*, Equation 9 ($R^2 = 0.696$). Indeed, the variables that significantly influenced the IRI progression were capable of developing IRI prediction models of high accuracy [87, 101]. An individual analysis of Equation 10 underlined that conclusion because the variable *PaveType* was separately included, rather than in combination with quantitative variables. In that model, the coefficients of the quantitative variables were an exact reflection of their effect on the dependent variable (IRI). The coefficients for *RealAge* and *TotalHVeh* were positive, indicating that higher values resulted in greater pavement deterioration, as with other models in the literature [19, 118]. Conversely, the coefficient of *BitThick* was negative, thereby confirming the hypothesis that thicker pavement layers require more time (or loads) before deterioration leads to damage. Generally, there was a negative correlation between bituminous thickness and IRI, as indicated in previous studies [117, 118]. Besides, the values of *PaveType* indicated which pavement type showed better performance. If the same values were maintained for all the remaining variables (*BitThick*, *RealAge*, and *TotalHVeh*), the IRI value of the mixed pavements would be superior, with a difference of 0.74 m/km when compared to a semi-rigid pavement and more than 1.5 m/km when compared to a flexible pavement. These coefficients were logical and in accordance with the anticipated deterioration rate of pavements in accordance with the base material. Treated cement base materials show higher elastic moduli than untreated materials [101, 119] but lower than concrete in composite pavements [120, 121]. It was also noteworthy that the coefficients associated with each variable in Equation 10 were highly similar to those established for Equation 9. Thus, the improved accuracy was due to the introduction of *PaveType*, which also minimally adjusted the values of the other coefficients.

The analysis of Equation 11 yielded analogous findings. The positive coefficient associated with TotalHVeh and RealAge indicated a positive contribution to the IRI, whereas the negative coefficient associated with BitThick indicated a contribution to longer-lasting pavements. The coefficients follow the logical trend presented for Equation 10. Similarly, the coefficients associated with the qualitative variable illustrate the disparate performance of each pavement type. The values of PaveType in Equation 11 showed the same nature (positive or negative) as in Equation 10, with highly similar values. Furthermore, all the values of A were positive, indicating that the age of the pavement has a deteriorating effect on its performance. However, all those coefficients also demonstrated that the same quantity of heavy vehicles had the most detrimental effect on flexible pavements and the least detrimental on mixed pavements, in correspondence with the different modulus of elasticity of each material.

Unlike ML and ANN models, the exact influence of each factor in the model can be determined with the deterministic approach, which results in an equation that shows the exact relationship between the independent variable and the dependent variables. Although lower accuracy levels are generally obtained with deterministic models, the equations presented in this research demonstrate high determination coefficients, underlining that a transferable equation can forecast IRI progression with sufficient levels of accuracy.

It must be noted that the proposed models in no way suggest optimal M&R interventions; they can nevertheless be used to predict future pavement conditions based on projected traffic volumes over coming years. It means that the IRI values may be anticipated over a previously established threshold, and future expenditure can therefore be foreseen. Moreover, various repair strategies were implemented on the selected stretches of road, which were used for modelling. So, the models were capable of capturing various M&R activities which are usually carried out in the region. The evaluation of various future repair strategies may therefore be analysed.

Finally, the proposed models offer the added benefit of requiring only three or four input variables—pavement age, cumulative traffic volumes, and bituminous layer thickness—which are typically collected by highway agencies. In comparison to models such as the MEPDG, developed by AASHTO [84, 85, 100], which require up to nine input variables, our models are more efficient, easier to implement, and deliver higher accuracy. The data collected in Gipuzkoa could not be evaluated using the MEPDG models because most of the required variables were not available in the PCG's Pavement Management System (PMS). This limitation was one of the main reasons the PCG needed to develop its own customized models. Moreover, our models could not be applied to data from other regions in Spain due to the lack of IRI (International Roughness Index) values for freeways. As previously mentioned, very few models exist for predicting IRI evolution on motorway lanes, and no other highway agencies were able to provide the specific data needed for applying our models.

5. Conclusion

Pavement performance models have become a key element of any Pavement Management System (PMS), due to their ability to predict future pavement conditions as a function of some known (or estimated) values. All highway agencies therefore need to further the development and practical use of a PMS. The Provincial Council of Gipuzkoa (PCG) manages the entire interurban road network in the province of Gipuzkoa, Spain, including the motorways (freeways) connecting to other regions and to France. The PCG PMS includes annual traffic volumes and the pavement structure obtained from the original and the M&R projects. International Roughness Index (IRI) data are collected throughout the network to assess pavement conditions. On dual carriageways, such as motorways, IRI values are collected on the right-hand lane of each carriageway, the most heavily trafficked lane, on both the right and left wheel paths. The literature review has shown that very few models have been proposed for motorways. Moreover, those models have generally been developed for a specific pavement type: either flexible, or rigid, or semi-rigid, or composite pavements. A deterministic approach to pavement deterioration modelling has therefore been followed on the basis of the available information.

A deterministic IRI performance prediction model of sufficient accuracy with fewer variables than other more complex models has been developed in this study. The models have been used to predict the future IRI for the right-hand lanes of motorways with the three above-mentioned pavement types within Gipuzkoa: flexible, semi-rigid, and composite pavements. Firstly, a simple multiple linear regression model was proposed based on only three variables, including pavement age, the total number of heavy vehicles passing through the section, and the total thickness of the bituminous layers, achieving a coefficient of determination (R^2) of 0.696. Introducing an additional qualitative variable, pavement type (including the three available types), the accuracy increased, and two more generalised linear models were presented. Using those four variables, R^2 of 0.781 and 0.795 were obtained. As can be seen, this accuracy exceeds the accuracy of MEPDG models specified in the AASHTO [84-85, 100], which require nine variables.

Furthermore, deterministic models directly show the exact relationships between the variables. Thus, the signs of the coefficients of the variables underline the effect of each one upon changes to the IRI. Pavement age and the total number of heavy vehicles contributed to higher rates of deterioration (observed as higher IRI values), and the thickness of the bituminous layers helped to reduce deterioration. The variable 'pavement type' clearly showed the different behaviour of the pavements. All other variables being equal, composite pavements had lower IRI values, while flexible pavements had greater deterioration. Semi-rigid pavements acted as an intermediate value between both types. The models reflected the different load distributions and, hence, the different performance levels and behaviours, which in turn underlined their validity.

6. Declarations

6.1. Author Contributions

Conceptualization, H.P.A., M.I., and I.G.; methodology, H.P.A. and I.G.; software, H.P.A., I.G., and Á.S.S.; validation, H.P.A., I.G., and Á.A.S.; formal analysis, H.P.A., M.I., and Á.A.S.; investigation, H.P.A. and M.I.; resources, M.I. and Á.A.S.; data curation, H.P.A., M.I., I.G.G., and Á.S.S.; writing—original draft preparation, H.P.A., I.G., and I.G.; writing—review and editing, H.P.A., I.G., and Á.S.S.; visualization, M.I. and Á.S.S.; supervision, H.P.A., I.G., and Á.S.S.; project administration, M.I. and I.G.; funding acquisition, H.P.A., M.I., and I.G. All authors have read and agreed to the published version of the manuscript.

6.2. Data Availability Statement

The data presented in this study are available on request from the corresponding author.

6.3. Funding

This research was funded by Gipuzkoako Foru Aldundia/Diputación Foral de Gipuzkoa (Provincial Council of Gipuzkoa), grant number P9, Project ‘Gipuzkoan eraikuntza eta mugikortasun adimentsu eta jasangarria/Construcción y movilidad inteligentes y sostenibles en Gipuzkoa’ of the Etorkizuna Eraikiz program 2022, and grant number P10; Project ‘MUGI JASS (MUGikortasuna Gipuzkoan: Interkonektatua, JASangarria eta Segurua/Movilidad en Gipuzkoa: interconectada, sostenible y segura)’ of the Etorkizuna Eraikiz program 2024; and the University of the Basque Country (UPV/EHU), grant GIU21/046.

6.4. Conflicts of Interest

The authors declare no conflict of interest.

7. References

- [1] Gautam, P. K., Kalla, P., Jethoo, A. S., Agrawal, R., & Singh, H. (2018). Sustainable use of waste in flexible pavement: A review. *Construction and Building Materials*, 180, 239–253. doi:10.1016/j.conbuildmat.2018.04.067.
- [2] Mulungye, R. M., Owende, P. M. O., & Mellon, K. (2007). Finite element modelling of flexible pavements on soft soil subgrades. *Materials and Design*, 28(3), 739–756. doi:10.1016/j.matdes.2005.12.006.
- [3] Huang, Y., Bird, R. N., & Heidrich, O. (2007). A review of the use of recycled solid waste materials in asphalt pavements. *Resources, Conservation and Recycling*, 52(1), 58–73. doi:10.1016/j.resconrec.2007.02.002.
- [4] Riaz, A., Yasir, N., Badin, G., & Mahmood, Y. (2024). Innovative Pavement Solutions: A Comprehensive Review from Conventional Asphalt to Sustainable Colored Alternatives. *Infrastructures*, 9(10), 186. doi:10.3390/infrastructures9100186.
- [5] Ullidtz, P. (1987). *Pavement Analysis. Developments in Civil Engineering*. Elsevier, Amsterdam, Netherlands.
- [6] Fedrigo, W., Visser, A. T., Steyn, W. J. M., & Núñez, W. P. (2021). Flexural behaviour of lightly cement stabilised materials: South Africa and Brazil. *Road Materials and Pavement Design*, 22(2), 397–422. doi:10.1080/14680629.2019.1634637.
- [7] Xu, J., Li, N., & Xu, T. (2022). Temperature Changes of Interlaminar Bonding Layer in Different Seasons and Effects on Mechanical Properties of Asphalt Pavement. *International Journal of Pavement Research and Technology*, 15(3), 589–605. doi:10.1007/s42947-021-00039-9.
- [8] Huhtala, M., Pihlajamäki, J., & Pienimäki, M. (1989). Effects of tires and tire pressures on road pavements. *Transportation Research Record*, 1227(1227), 107–114.
- [9] Tingle, J. S., Newman, J. K., Larson, S. L., Weiss, C. A., & Rushing, J. F. (2007). Stabilization mechanisms of nontraditional additives. *Transportation Research Record*, 2(1989), 59–67. doi:10.3141/1989-49.
- [10] Shon, C. S., Saylak, D., & Mishra, S. K. (2010). Combined use of calcium chloride and fly ash in road base stabilization. *Transportation Research Record*, 2186, 120–129. doi:10.3141/2186-13.
- [11] Linares-Unamunzaga, A., Gonzalo-Orden, H., Minguela, J. D., & Pérez-Acebo, H. (2018). New procedure for compacting prismatic specimens of cement-treated base materials. *Applied Sciences (Switzerland)*, 8(6), 970. doi:10.3390/app8060970.
- [12] Osorio-Lird, A., Chamorro, A., & González, Á. (2021). Analysis of roughness performance of chloride-stabilised rural roads. *International Journal of Pavement Engineering*, 22(13), 1720–1730. doi:10.1080/10298436.2020.1721496.
- [13] Diniz, B. C., Fedrigo, W., Kleinert, T. R., Batista, G. dos S., Núñez, W. P., Correa, B. M., & Brito, L. A. T. (2024). Lime Stabilization of Tropical Soil for Resilient Pavements: Mechanical, Microscopic, and Mineralogical Characteristics. *Materials*, 17(19), 4720. doi:10.3390/ma17194720.

- [14] Linares-Unamunzaga, A., Pérez-Acebo, H., Rojo, M., & Gonzalo-Orden, H. (2019). Flexural strength prediction models for soil-cement from Unconfined Compressive Strength at Seven Days. *Materials*, 12(3), 387. doi:10.3390/ma12030387.
- [15] Li, Q., Wang, Z., Li, Y., & Shang, J. (2018). Cold recycling of lime-fly ash stabilized macadam mixtures as pavement bases and subbases. *Construction and Building Materials*, 169, 306–314. doi:10.1016/j.conbuildmat.2018.03.030.
- [16] Dong, Q., Zhao, X., Chen, X., Ma, X., & Cui, X. (2021). Long-term mechanical properties of in situ semi-rigid base materials. *Road Materials and Pavement Design*, 22(7), 1692–1707. doi:10.1080/14680629.2019.1710239.
- [17] Lv, S., Xia, C., Liu, H., You, L., Qu, F., Zhong, W., Yang, Y., & Washko, S. (2021). Strength and fatigue performance for cement-treated aggregate base materials. *International Journal of Pavement Engineering*, 22(6), 690–699. doi:10.1080/10298436.2019.1634808.
- [18] Yu, L., Wu, Y., Meng, Y., Huang, G., Li, R., & Pei, J. (2023). Study on fatigue crack propagation failure in semi-rigid base. *Construction and Building Materials*, 409, 134007. doi:10.1016/j.conbuildmat.2023.134007.
- [19] Khattak, M. J., Nur, M. A., Bhuyan, M. R. U. K., & Gaspard, K. (2014). International roughness index models for HMA overlay treatment of flexible and composite pavements. *International Journal of Pavement Engineering*, 15(4), 334–344. doi:10.1080/10298436.2013.842237.
- [20] Chen, C., Williams, R. C., Marasinghe, M. G., Ashlock, J. C., Smadi, O., Schram, S., & Buss, A. (2015). Assessment of composite pavement performance by survival analysis. *Journal of Transportation Engineering*, 141(9), 04015018. doi:10.1061/(ASCE)TE.1943-5436.0000784.
- [21] Pérez-Acebo, H., Montes-Redondo, M., Appelt, A., & Findley, D. J. (2023). A simplified skid resistance predicting model for a freeway network to be used in a pavement management system. *International Journal of Pavement Engineering*, 24(2), 2020266. doi:10.1080/10298436.2021.2020266.
- [22] Salas, M. Á., Pérez-Acebo, H., Calderón, V., & Gonzalo-Orden, H. (2018). Bitumen modified with recycled polyurethane foam for employment in hot mix asphalt. *Ingenieria e Investigacion*, 38(1), 60–66. doi:10.15446/ing.investig.v38n1.65631.
- [23] Zeiada, W., Hamad, K., Omar, M., Underwood, B. S., Khalil, M. A., & Karzad, A. S. (2019). Investigation and modelling of asphalt pavement performance in cold regions. *International Journal of Pavement Engineering*, 20(8), 986–997. doi:10.1080/10298436.2017.1373391.
- [24] Zeiada, W., Dabous, S. A., Hamad, K., Al-Ruzouq, R., & Khalil, M. A. (2020). Machine Learning for Pavement Performance Modelling in Warm Climate Regions. *Arabian Journal for Science and Engineering*, 45(5), 4091–4109. doi:10.1007/s13369-020-04398-6.
- [25] Naseri, H., Jahanbakhsh, H., Foomajd, A., Galustanian, N., Karimi, M. M., & D. Waygood, E. O. (2023). A newly developed hybrid method on pavement maintenance and rehabilitation optimization applying Whale Optimization Algorithm and random forest regression. *International Journal of Pavement Engineering*, 24(2), 2147672. doi:10.1080/10298436.2022.2147672.
- [26] Shokoohi, M., Golroo, A., & Ardeshtari, A. (2023). Pavement maintenance planning using a risk-based approach and fault tree analysis. *International Journal of Pavement Engineering*, 24(2), 2276160. doi:10.1080/10298436.2023.2276160.
- [27] Sandamal, K., Shashiprabha, S., Muttill, N., & Rathnayake, U. (2023). Pavement Roughness Prediction Using Explainable and Supervised Machine Learning Technique for Long-Term Performance. *Sustainability (Switzerland)*, 15(12), 9617. doi:10.3390/su15129617.
- [28] Kulkarni, R. B., & Miller, R. W. (2003). Pavement Management Systems: Past, Present, and Future. *Transportation Research Record*, 1853(1853), 65–71. doi:10.3141/1853-08.
- [29] Santos, J., & Ferreira, A. (2012). Pavement design optimization considering costs and preventive interventions. *Journal of Transportation Engineering*, 138(7), 911–923. doi:10.1061/(ASCE)TE.1943-5436.0000390.
- [30] Gomes Correia, M., Bonates, T. de O. e., Prata, B. de A., & Nobre Júnior, E. F. (2022). An integer linear programming approach for pavement maintenance and rehabilitation optimization. *International Journal of Pavement Engineering*, 23(8), 2710–2727. doi:10.1080/10298436.2020.1869736.
- [31] Yao, L., Leng, Z., Jiang, J., & Ni, F. (2022). Modelling of pavement performance evolution considering uncertainty and interpretability: a machine learning based framework. *International Journal of Pavement Engineering*, 23(14), 5211–5226. doi:10.1080/10298436.2021.2001814.
- [32] AASHTO. (1993). *AASHTO Guide for design of pavement structures*. American Association of State Highway and Transportation Officials, Washington, United States.
- [33] Pérez-Acebo, H., Mindra, N., Railean, A., & Rojí, E. (2019). Rigid pavement performance models by means of Markov Chains with half-year step time. *International Journal of Pavement Engineering*, 20(7), 830–843. doi:10.1080/10298436.2017.1353390.

- [34] Wu, Z., Flintsch, G., Ferreira, A., & de Picado-Santos, L. (2012). Framework for multiobjective optimization of physical highway assets investments. *Journal of Transportation Engineering*, 138(12), 1411–1421. doi:10.1061/(ASCE)TE.1943-5436.0000458.
- [35] Khan, M. U., Mesbah, M., Ferreira, L., & Williams, D. J. (2016). Development of optimum pavement maintenance strategies for a road network. *Australian Journal of Civil Engineering*, 14(2), 85–96. doi:10.1080/14488353.2017.1362823.
- [36] Odoki, J. B., & Kerali, H. G. (2000). Analytical framework and model descriptions. *HDM 4: Highway Development & Management Series*, 4, 1–627.
- [37] Liu, Q., Xie, J., & Zhang, Z. (2021). A Vehicle Fuel Consumption Model on Reconstructed Roads Based on the Roughness and Its Measurement Method. *Advances in Civil Engineering*, 8812376. doi:10.1155/2021/8812376.
- [38] Fani, A., Golroo, A., Ali Mirhassani, S., & Gandomi, A. H. (2022). Pavement maintenance and rehabilitation planning optimisation under budget and pavement deterioration uncertainty. *International Journal of Pavement Engineering*, 23(2), 414–424. doi:10.1080/10298436.2020.1748628.
- [39] Zhang, Z., Zhang, H., Xu, S., & Lv, W. (2022). Pavement roughness evaluation method based on the theoretical relationship between acceleration measured by smartphone and IRI. *International Journal of Pavement Engineering*, 23(9), 3082–3098. doi:10.1080/10298436.2021.1881783.
- [40] Levesque, W., Samson, N., Bégin-Drolet, A., & Lépine, J. (2023). Pavement-effects on heavy-vehicle fuel consumption in cold climate using a statistical approach. *Transportation Research Part D: Transport and Environment*, 120. doi:10.1016/j.trd.2023.103792.
- [41] Tamagusko, T., & Ferreira, A. (2023). Machine Learning for Prediction of the International Roughness Index on Flexible Pavements: A Review, Challenges, and Future Directions. *Infrastructures*, 8(12), 170. doi:10.3390/infrastructures8120170.
- [42] Sayers, M., Gillespie, T. D., & Queiroz, C. A. V. (1984). International Experiment to Establish Correlation and Standard Calibration Methods for Road Roughness Measurements. The World Bank, Washington, United States.
- [43] Sayers, M. W. (1995). On the calculation of international roughness index from longitudinal road profile. *Transportation Research Record*, Washington, United States.
- [44] Sayers, M. W., Gillespie, T. D., & Paterson, W. D. O. (1986). Guidelines for Conducting and Calibrating Road Roughness Measurements. World Bank Technical Paper Number 46, The World Bank, Washington, United States.
- [45] Múčka, P. (2017). International Roughness Index specifications around the world. *Road Materials and Pavement Design*, 18(4), 929–965. doi:10.1080/14680629.2016.1197144.
- [46] Lin, J. D., Yau, J. T., & Hsiao, L. H. (2003). Correlation analysis between international roughness index (IRI) and pavement distress by neural network. 82nd Annual Meeting of the Transportation Research Board, 12-16, January, 2003, Washington, United States.
- [47] Yamany, M. S., Saeed, T. U., Volovski, M., & Ahmed, A. (2020). Characterizing the Performance of Interstate Flexible Pavements Using Artificial Neural Networks and Random Parameters Regression. *Journal of Infrastructure Systems*, 26(2), 04020010. doi:10.1061/(asce)is.1943-555x.0000542.
- [48] Sidess, A., Ravina, A., & Oged, E. (2022). A model for predicting the deterioration of the international roughness index. *International Journal of Pavement Engineering*, 23(5), 1393–1403. doi:10.1080/10298436.2020.1804062.
- [49] Alonso-Solorzano, Á., Pérez-Acebo, H., Findley, D. J., & Gonzalo-Orden, H. (2023). Transition probability matrices for pavement deterioration modelling with variable duty cycle times. *International Journal of Pavement Engineering*, 24(2), 2278694. doi:10.1080/10298436.2023.2278694.
- [50] Pérez-Acebo, H., Bejan, S., & Gonzalo-Orden, H. (2018). Transition Probability Matrices for Flexible Pavement Deterioration Models with Half-Year Cycle Time. *International Journal of Civil Engineering*, 16(9), 1045–1056. doi:10.1007/s40999-017-0254-z.
- [51] Gharieb, M., Nishikawa, T., Nakamura, S., & Thepvongsa, K. (2022). Modeling of Pavement Roughness Utilizing Artificial Neural Network Approach for Laos National Road Network. *Journal of Civil Engineering and Management*, 28(4), 261–277. doi:10.3846/jcem.2022.15851.
- [52] Isradi, M., Rifai, A. I., Prasetijo, J., Kinasih, R. K., & Setiawan, M. I. (2024). Development of Pavement Deterioration Models Using Markov Chain Process. *Civil Engineering Journal (Iran)*, 10(9), 2954–2965. doi:10.28991/CEJ-2024-010-09-012.
- [53] Boonsiripant, S., Athan, C., Jedwanna, K., Lertworawanich, P., & Sawangsuriya, A. (2024). Comparative Analysis of Deep Neural Networks and Graph Convolutional Networks for Road Surface Condition Prediction. *Sustainability (Switzerland)*, 16(22), 9805. doi:10.3390/su16229805.

- [54] AASHTO. (2012). *Pavement Management Guide (2nd Ed.)*. American Association of State Highway and Transportation Officials (AASHTO), Washington, United States.
- [55] Hudson, W. R., Haas, R., & Pedigo, R. D. (1979). *Pavement Management System Development*. National Cooperative Highway Research Program Report 2015, Highway Research Record 407, Transportation Research Board, National Research Council, Washington, United States.
- [56] Saplioglu, M., Unal, A., & Bocek, M. (2022). Detection of critical road roughness sections by trend analysis and investigation of driver speed interaction. *Frontiers of Structural and Civil Engineering*, 16(4), 515–532. doi:10.1007/s11709-022-0814-4.
- [57] Haas, R., Hudson, W. R., & Zaniewski, J. P. (1994). *Modern pavement management*. Krieger Publishing Company, Melbourne, United States.
- [58] Uddin, W. (2005). *Pavement Management Systems*. The Handbook of Highway Engineering, CRC Press, Boca Raton, United States. doi:10.1201/9781420039504.ch18.
- [59] Justo-Silva, R., Ferreira, A., & Flintsch, G. (2021). Review on machine learning techniques for developing pavement performance prediction models. *Sustainability (Switzerland)*, 13(9), 5248. doi:10.3390/su13095248.
- [60] Abaza, K. A. (2018). Empirical-Markovian model for predicting the overlay design thickness for asphalt concrete pavement. *Road Materials and Pavement Design*, 19(7), 1617–1635. doi:10.1080/14680629.2017.1338188.
- [61] Sharma, A., Sachdeva, S. N., & Aggarwal, P. (2023). Predicting IRI Using Machine Learning Techniques. *International Journal of Pavement Research and Technology*, 16(1), 128–137. doi:10.1007/s42947-021-00119-w.
- [62] Wu, Y., Pang, Y., & Zhu, X. (2024). Evolution of prediction models for road surface irregularity: Trends, methods and future. *Construction and Building Materials*, 449, 138316. doi:10.1016/j.conbuildmat.2024.138316.
- [63] Park, S. H., & Kim, J. H. (2019). Comparative Analysis of Performance Prediction Models for Flexible Pavements. *Journal of Transportation Engineering, Part B: Pavements*, 145(1), 04018062. doi:10.1061/jpeodx.0000090.
- [64] Dong, Q., Huang, B., & Richards, S. H. (2015). Calibration and application of treatment performance models in a pavement management system in Tennessee. *Journal of Transportation Engineering*, 141(2), 04014076. doi:10.1061/(ASCE)TE.1943-5436.0000738.
- [65] Amador-Jiménez, L. E., & Mrawira, D. (2011). Reliability-based initial pavement performance deterioration modelling. *International Journal of Pavement Engineering*, 12(2), 177–186. doi:10.1080/10298436.2010.535538.
- [66] Elhadidy, A. A., Elbeltagi, E. E., & El-Badawy, S. M. (2020). Network-Based Optimization System for Pavement Maintenance Using a Probabilistic Simulation-Based Genetic Algorithm Approach. *Journal of Transportation Engineering, Part B: Pavements*, 146(4), 04020069. doi:10.1061/jpeodx.0000237.
- [67] García-Segura, T., Montalbán-Domingo, L., Llopis-Castelló, D., Lepech, M. D., Sanz, M. A., & Pellicer, E. (2022). Incorporating pavement deterioration uncertainty into pavement management optimization. *International Journal of Pavement Engineering*, 23(6), 2062–2073. doi:10.1080/10298436.2020.1837827.
- [68] Li, N., Haas, R., & Xie, W. C. (1997). Development of a new asphalt pavement performance prediction model. *Canadian Journal of Civil Engineering*, 24(4), 547–559. doi:10.1139/197-001.
- [69] Abaza, K. A. (2016). Back-calculation of transition probabilities for Markovian-based pavement performance prediction models. *International Journal of Pavement Engineering*, 17(3), 253–264. doi:10.1080/10298436.2014.993185.
- [70] Yamany, M. S., Abraham, D. M., & Labi, S. (2021). Comparative Analysis of Markovian Methodologies for Modeling Infrastructure System Performance. *Journal of Infrastructure Systems*, 27(2), 04021003. doi:10.1061/(asce)is.1943-555x.0000604.
- [71] Alimoradi, S., Golroo, A., & Asgharzadeh, S. M. (2022). Development of pavement roughness master curves using Markov Chain. *International Journal of Pavement Engineering*, 23(2), 453–463. doi:10.1080/10298436.2020.1752917.
- [72] Alaswadko, N., & Hwayyis, K. (2022). An approach to investigate the supplementary inconsistency between time series data for predicting road pavement performance models. *International Journal of Pavement Engineering*, 24(2), 2045017. doi:10.1080/10298436.2022.2045017.
- [73] Gong, H., Sun, Y., Hu, W., Polaczyk, P. A., & Huang, B. (2019). Investigating impacts of asphalt mixture properties on pavement performance using LTPP data through random forests. *Construction and Building Materials*, 204, 203–212. doi:10.1016/j.conbuildmat.2019.01.198.
- [74] Aljarah, I., Faris, H., & Mirjalili, S. (2018). Optimizing connection weights in neural networks using the whale optimization algorithm. *Soft Computing*, 22(1), 1–15. doi:10.1007/s00500-016-2442-1.

- [75] Mishra, R., Gupta, H. P., & Dutta, T. (2021). A Road Health Monitoring System Using Sensors in Optimal Deep Neural Network. *IEEE Sensors Journal*, 21(14), 15527–15534. doi:10.1109/JSEN.2020.3005998.
- [76] Elshaboury, N., Yamany, M. S., Labi, S., & Smadi, O. (2024). Enhancing local road pavement condition prediction using Bayesian-optimized ensemble machine learning and adaptive synthetic sampling technique. *International Journal of Pavement Engineering*, 25(1), 2365957. doi:10.1080/10298436.2024.2365957.
- [77] Sollazzo, G., Fwa, T. F., & Bosurgi, G. (2017). An ANN model to correlate roughness and structural performance in asphalt pavements. *Construction and Building Materials*, 134, 684–693. doi:10.1016/j.conbuildmat.2016.12.186.
- [78] García de Soto, B., Bumbacher, A., Deublein, M., & Adey, B. T. (2018). Predicting road traffic accidents using artificial neural network models. *Infrastructure Asset Management*, 5(4), 132–144. doi:10.1680/jinam.17.00028.
- [79] AASHTO. (1962). *The AASHTO Road Test: Pavement research*. Washington, DC: National Academy of Sciences - National Research Council, American Association of State Highway and Transportation Officials (AASHTO), Washington, United States.
- [80] Watanatada, T., Harral, C. G., Paterson, W. D. O., Dhareshwar, A. M., Bhandari, A., & Tsunokawa, K. (1990). *The highway design and maintenance standards model. Volume 1. Description of the HDM-III model. Transportation Research Part A: General*. John Hopkins University Press, Maryland, United States.
- [81] Morosiuk, G., Riley, M. J., & Odoki, J. B. (2004). *Modelling road deterioration and works effects-version 2-Highway Development and Management-HDM-4*. Highway development and management series, The World Bank, Washington, United States.
- [82] Paterson, W. D. O. (1990). *Road deterioration and maintenance effects: Models for planning and management. In Transportation Research Part A: General*. John Hopkins University Press, Maryland, United States. doi:10.1016/0191-2607(90)90027-4.
- [83] Pérez-Acebo, H., Linares-Unamunzaga, A., Abejón, R., & Rojí, E. (2018). Research trends in pavement management during the first years of the 21st century: A bibliometric analysis during the 2000-2013 Period. *Applied Sciences (Switzerland)*, 8(7), 1041. doi:10.3390/app8071041.
- [84] AASHTO. (2008). *Mechanistic-Empirical Pavement Design Guide. A manual of practice*. American Association of State Highway and Transportation Officials (AASHTO), Washington, United States.
- [85] AASHTO. (2015). *Mechanistic-Empirical Pavement Design Guide. A manual of practice (2nd Ed.)*. American Association of State Highway and Transportation Officials (AASHTO), Washington, United States.
- [86] AASHTO. (2004). *Guide for Mechanistic-Empirical design of new and rehabilitated pavement structures; NCHRP 1-37A*. American Association of State Highway and Transportation Officials (AASHTO), Washington, United States.
- [87] Abdelaziz, N., Abd El-Hakim, R. T., El-Badawy, S. M., & Afify, H. A. (2020). International Roughness Index prediction model for flexible pavements. *International Journal of Pavement Engineering*, 21(1), 88–99. doi:10.1080/10298436.2018.1441414.
- [88] Pérez-Acebo, H., Linares-Unamunzaga, A., Rojí, E., & Gonzalo-Orden, H. (2020). IRI performance models for flexible pavements in two-lane roads until first maintenance and/or rehabilitation work. *Coatings*, 10(2), 97. doi:10.3390/coatings10020097.
- [89] Moreira, A. V., Tinoco, J., Oliveira, J. R. M., & Santos, A. (2018). An application of Markov chains to predict the evolution of performance indicators based on pavement historical data. *International Journal of Pavement Engineering*, 19(10), 937–948. doi:10.1080/10298436.2016.1224412.
- [90] Alaswadko, N., Hassan, R., Meyer, D., & Mohammed, B. (2019). Modelling roughness progression of sealed granular pavements: a new approach. *International Journal of Pavement Engineering*, 20(2), 222–232. doi:10.1080/10298436.2017.1283689.
- [91] Naseri, H., Ehsani, M., Golroo, A., & Moghadas Nejad, F. (2022). Sustainable pavement maintenance and rehabilitation planning using differential evolutionary programming and coyote optimisation algorithm. *International Journal of Pavement Engineering*, 23(8), 2870–2887. doi:10.1080/10298436.2021.1873331.
- [92] Marcelino, P., de Lurdes Antunes, M., Fortunato, E., & Gomes, M. C. (2021). Machine learning approach for pavement performance prediction. *International Journal of Pavement Engineering*, 22(3), 341–354. doi:10.1080/10298436.2019.1609673.
- [93] Kaloop, M. R., El-Badawy, S. M., Ahn, J., Sim, H. B., Hu, J. W., & Abd El-Hakim, R. T. (2022). A hybrid wavelet-optimally-pruned extreme learning machine model for the estimation of international roughness index of rigid pavements. *International Journal of Pavement Engineering*, 23(3), 862–876. doi:10.1080/10298436.2020.1776281.
- [94] Choi, S., & Do, M. (2020). Development of the road pavement deterioration model based on the deep learning method. *Electronics (Switzerland)*, 9(1), 3. doi:10.3390/electronics9010003.

- [95] Nguyen, H. L., Pham, B. T., Son, L. H., Thang, N. T., Ly, H. B., Le, T. T., Ho, L. S., Le, T. H., & Bui, D. T. (2019). Adaptive network based fuzzy inference system with meta-heuristic optimizations for international roughness index prediction. *Applied Sciences (Switzerland)*, 9(21), 4715. doi:10.3390/app9214715.
- [96] Yang, L., Hu, Y., & Zhang, H. (2020). Comparative study on asphalt pavement rut based on analytical models and test data. *International Journal of Pavement Engineering*, 21(6), 781–795. doi:10.1080/10298436.2018.1511781.
- [97] Guo, R., Nian, T., Li, P., Fu, J., & Guo, H. (2019). Anti-erosion performance of asphalt pavement with a sub-base of cement-treated mixtures. *Construction and Building Materials*, 223, 278–287. doi:10.1016/j.conbuildmat.2019.06.202.
- [98] Wang, X., & Zhong, Y. (2019). Reflective crack in semi-rigid base asphalt pavement under temperature-traffic coupled dynamics using XFEM. *Construction and Building Materials*, 214, 280–289. doi:10.1016/j.conbuildmat.2019.04.125.
- [99] Yan, X., Chen, L., You, Q., & Fu, Q. (2019). Experimental analysis of thermal conductivity of semi-rigid base asphalt pavement. *Road Materials and Pavement Design*, 20(5), 1215–1227. doi:10.1080/14680629.2018.1431147.
- [100] AASHTO. (2020). *Mechanistic-Empirical Pavement Design Guide. A manual of practice (3rd Ed.)*. American Association of State Highway and Transportation Officials (AASHTO), Washington, United States.
- [101] Pérez-Acebo, H., Gonzalo-Orden, H., Findley, D. J., & Rojí, E. (2021). Modeling the international roughness index performance on semi-rigid pavements in single carriageway roads. *Construction and Building Materials*, 272, 121665. doi:10.1016/j.conbuildmat.2020.121665.
- [102] Hanson, J. R. (2006). *Cracking and Roughness of Asphalt Pavements Constructed Using Cement-Treated Base Materials*. Master Thesis, Brigham Young University, Provo, United States.
- [103] Assogba, O. C., Tan, Y., Zhou, X., Zhang, C., & Anato, J. N. (2020). Numerical investigation of the mechanical response of semi-rigid base asphalt pavement under traffic load and nonlinear temperature gradient effect. *Construction and Building Materials*, 235, 117406. doi:10.1016/j.conbuildmat.2019.117406.
- [104] Barros, R., Yasarer, H., Uddin, W., & Sultana, S. (2021). Roughness Modeling for Composite Pavements using Machine Learning. *IOP Conference Series: Materials Science and Engineering*, 1203(3), 032035. doi:10.1088/1757-899x/1203/3/032035.
- [105] Barros, R., Yasarer, H., & Sultana, S. (2022). International Roughness Index Model for Composite Pavements in the LTPP Wet Non-Freeze Climate Region: Machine Learning and Regression Approaches. 101st Annual Meeting of the Transportation Research Board (TRB), 9-13 January, 2022, Washington, United States.
- [106] Neema, I. (2020). *Cluster-Based Composite Pavement Deterioration Modeling: A Framework for Incorporating Flooding*. Master Thesis, The University of North Carolina at Charlotte, Charlotte, United States.
- [107] Kaya, O., Ceylan, H., Kim, S., Waid, D., & Moore, B. P. (2020). Statistics and Artificial Intelligence-Based Pavement Performance and Remaining Service Life Prediction Models for Flexible and Composite Pavement Systems. *Transportation Research Record*, 2674(10), 448–460. doi:10.1177/0361198120915889.
- [108] Al-Suleiman, T. I., & Shiyab, A. M. S. (2003). Prediction of Pavement Remaining Service Life Using Roughness Data - Case Study in Dubai. *International Journal of Pavement Engineering*, 4(2), 121–129. doi:10.1080/10298430310001634834.
- [109] Georgiou, P., Plati, C., & Loizos, A. (2018). Soft Computing Models to Predict Pavement Roughness: A Comparative Study. *Advances in Civil Engineering*, 2018. doi:10.1155/2018/5939806.
- [110] DFG/GFA (2024). Road capacity information for Gipuzkoa. Compilation up to 2023. Dep. de Infraestructuras Viarias y Estrategia Territorial, Donostia-San Sebastián, Spain. (In Spanish).
- [111] MFOM (Ministerio de Fomento). (2003). FOM/3460/2003, of November 28, approving standard 6.1-IC "Road Sections" of the Highway Instructions. Ministerio de Fomento, Madrid, Spain. (In Spanish).
- [112] Hwang, Y., & Song, J. (2023). Recent deep learning methods for tabular data. *Communications for Statistical Applications and Methods*, 30(2), 215–226. doi:10.29220/CSAM.2023.30.2.215.
- [113] Borisov, V., Leemann, T., Sebler, K., Haug, J., Pawelczyk, M., & Kasneci, G. (2024). Deep Neural Networks and Tabular Data: A Survey. *IEEE Transactions on Neural Networks and Learning Systems*, 35(6), 7499–7519. doi:10.1109/TNNLS.2022.3229161.
- [114] Montgomery, D. C., Peck, E. A., & Vining, G. G. (2021). *Introduction to linear regression analysis*. John Wiley & Sons, Hoboken, United States.
- [115] Pérez-Acebo, H., Gonzalo-Orden, H., & Rojí, E. (2019). Skid resistance prediction for new two-lane roads. *Proceedings of the Institution of Civil Engineers: Transport*, 172(5), 264–273. doi:10.1680/jtran.17.00045.

- [116] Zhou, Q., Okte, E., & Al-Qadi, I. L. (2021). Predicting pavement roughness using deep learning algorithms. *Transportation Research Record*, 2675(11), 1062–1072. doi:10.1177/03611981211023765.
- [117] George, K. P. (2000). MDOT pavement management system: prediction models and feedback system (No. FHWA/MS-DOT-RD-00-119). Department of Transportation, Mississippi, United States.
- [118] Albuquerque, F., & Núñez, W. (2011). Development of roughness prediction models for low-volume road networks in Northeast Brazil. *Transportation Research Record*, 2205, 198–205. doi:10.3141/2205-25.
- [119] Zu, F., Du, C., Han, C., Xu, L., & Peng, Q. (2023). Applicable Conditions of Room-and-Pillar Mining Goaf Treatment Methods under a Traffic Load. *Applied Sciences (Switzerland)*, 13(3), 2024. doi:10.3390/app13032024.
- [120] Aragón, G., Pérez-Acebo, H., Salas, M. Á., & Aragón-Torre, Á. (2024). Analysis of the static and dynamic elastic moduli of a one-coat rendering mortar with laboratory and in situ samples. *Case Studies in Construction Materials*, 20. doi:10.1016/j.cscm.2024.e02868.
- [121] Han, S. H., & Kim, J. K. (2004). Effect of temperature and age on the relationship between dynamic and static elastic modulus of concrete. *Cement and Concrete Research*, 34(7), 1219–1227. doi:10.1016/j.cemconres.2003.12.011.